Molecular Biology of the Cell
Vol. 12, 2308–2327, August 2001

# Biogenesis of Golgi Stacks in Imaginal Discs of *Drosophila melanogaster*

**Vangelis Kondylis, Sarah E. Goulding, Jonathan C. Dunne, and Catherine Rabouille***

The Wellcome Trust Centre for Cell Biology, Institute of Cell and Molecular Biology, University of Edinburgh, Edinburgh, EH9 3JR, Scotland, United Kingdom

Submitted December 8, 2000; Revised April 5, 2001; Accepted June 4, 2001
Monitoring Editor: Vivek Malhotra

We provide a detailed description of Golgi stack biogenesis that takes place in vivo during one of the morphogenetic events in the lifespan of *Drosophila melanogaster*. In early third-instar larvae, small clusters consisting mostly of vesicles and tubules were present in epithelial imaginal disk cells. As larvae progressed through mid- and late-third instar, these larval clusters became larger but also increasingly formed cisternae, some of which were stacked. In white pupae, the typical Golgi stack was observed. We show that larval clusters are Golgi stack precursors by 1) localizing various Golgi-specific markers to the larval clusters by electron and immunofluorescence confocal microscopy, 2) driving this conversion in wild-type larvae incubated at 37°C for 2 h, and 3) showing that this conversion does not take place in an NSF1 mutant (*comt 17*). The biological significance of this conversion became clear when we found that the steroid hormone 20-hydroxyecdysone (ecdysone) is critically involved in this conversion. In its absence, Golgi stack biogenesis did not occur and the larval clusters remained unaltered. We showed that dGM130 and sec23p expression increases approximately three- and fivefold, respectively, when discs are exposed to ecdysone in vivo and in vitro. Taken together, these results suggest that we have developed an in vivo system to study the ecdysone-triggered Golgi stack biogenesis.

## INTRODUCTION

In eukaryotic cells, the Golgi apparatus consists of stacked flattened membrane-bound compartments called cisternae. Abutting each side of the stacks is a tubular/vesicular network, the *cis*- and *trans*-Golgi networks. How this architecture is built and maintained has recently been addressed by the development of in vitro and semi-intact cell assays. The in vitro assay measured the rebuilding of the Golgi apparatus from mitotic Golgi fragments (Rabouille *et al.*, 1995b). The semi-intact cell system visualized the rebuilding of the Golgi complex from illimaquinone-generated Golgi fragments (Acharya *et al.*, 1995). These assays have allowed the identification of several proteins involved in this rebuilding process, such as NEM sensitive factor (NSF) and its cofactor $\alpha$ soluble NSF attachment protein (a-SNAP) (Acharya *et al.*, 1995; Rabouille *et al.*, 1995a; Müller *et al.*, 1999), p97 (Acharya *et al.*, 1995; Rabouille *et al.*, 1995a), and its cofactor p47 (Kondo *et al.*, 1997). Syntaxin 5 was shown to interact with both fusion machineries (Rabouille *et al.*, 1998). p115 (Rabouille *et al.*, 1995a), Golgi matrix 130 (GM130) (Nakamura *et al.*, 1997), GRASP65 (Barr *et al.*, 1997), and GRASP55 (Shorter *et al.*, 1999) were shown to be involved.

* Corresponding author. E-mail address: C.Rabouille@ed.ac.uk.

Both in vitro assays were based on the reassembly of preexisting disassembled Golgi stacks. We therefore set out to characterize how Golgi apparatus grows and how stacked cisternae are formed in vivo. We used *Drosophila melanogaster* as a model organism primarily because it is readily amenable to genetics and cell biology. Several *Drosophila* tissues exhibit a Golgi apparatus with a morphology very similar to mammalian cells of stacked cisternae and networks of tubular membranes. The stacks are seemingly not linked to one another in a large ribbon that forms the single-copy organelle capping the nucleus typical of mammalian cells (Rabouille *et al.*, 1999). Instead, they remain dispersed throughout the cytoplasm. Several of the *Drosophila* genes encoding the proteins involved in Golgi organization have been cloned: dNSF1, one of the homologs of NSF (Ordway *et al.*, 1994; Pallanck *et al.*, 1995a); NSF2 (the other NSF homolog, Pallanck *et al.*, 1995b); TER94, one of the two homologs of p97 (Pinter *et al.*, 1998); Sed5, the homolog of syntaxin5 (Banfield *et al.*, 1994); and the *Drosophila* homolog of p115 (dp115) and GM130 (dGM130) (Adams *et al.*, 2000; Dunne and Rabouille, 2001). With the exception of TGN38/46 and giantin, almost all the known mammalian proteins related to the Golgi apparatus have homologs in *Drosophila* (Adams *et al.*, 2000; Dunne and Rabouille, 2001). Due to the large collection of mutants (EMS and P element

insertion, deletion, etc.), the study of these proteins has been made easier. This is particularly true for dNSF1 (*comt*; Siddiqi and Benzer, 1976), TER94 (Leon and McKearin, 1999), and sed5 (Ashburner *et al.*, 1999).

The first step in investigating the possible role of these proteins in Golgi stack biogenesis with the use of *Drosophila* genetics was to describe a developmental event during which the Golgi stack would acquire its typical morphology of stacked cisternae. We focused on the elongation of the leg and wing imaginal discs that takes place between the stages of early third-instar larvae and puparium formation (white pupae). Leg imaginal discs begin as concentrically folded flat sac-like structures that will give rise to adult legs. They comprise two epithelial cell layers. One is a squamous thin epithelium (peripodial membrane), the other is folded and comprises columnar cells (5 $\mu$m in diameter and up to 30 $\mu$m in height) (Fristrom and Fristrom, 1993). The binding of the steroid hormone 20-hydroxyecdysone (ecdysone) to its nuclear receptors in the disc epithelial cells during late third-instar larvae induces the more peripheral folds to constrict, pushing the central folds toward the peripodium. As a consequence leg discs lose their flattened shape and elongate (von Kalm *et al.*, 1995). Wing discs expand in a similar manner (Fristrom and Fristrom, 1993). This first phase of disc elongation is completed at puparium formation.

We show here that this organogenesis is accompanied by the biogenesis of the Golgi stacks starting with small larval clusters of vesicles and tubules in early third-instar larvae, to larger clusters that contain Golgi markers in mid- and late third-instar larvae followed by the formation of stacks of cisternae in white pupae. We show that the larval clusters contain Golgi proteins, that their conversion into Golgi stack is dependent on dNSF1, and is triggered by ecdysone.

## MATERIALS AND METHODS

### *WT Larvae*

The $W^{1118}$ and OregonR stocks were obtained from Andrew Jarman's lab (Edinburgh, Scotland) and were both referred to as wild type (WT). They were maintained at 22°C. Early third-instar larvae were defined as those larvae that have the characteristics of a third-instar larvae (size, mouthhook, fanned anterior spiracles) but that are still burrowed in the food. Mid-third-instar larvae were defined as third-instar larvae free of the food and still wandering. The motionless third-instar larvae were late third-instar larvae. They also have swollen salivary glands and darkened everted spiracles. White pupae are the young pupae that have a white pupal case.

### *Fly Stocks and Experiments*

*comt 17* stock (gift from Barry Gunetsky, Madison, WI) is a thermosensitive allele of dNSF1 that is localized on the first chromosome. At 37°C, dNSF1 is misfolded and nonfunctional (Siddiqi and Benzer, 1976; Pallanck *et al.*, 1995a). HSN is a transgene comprising dNSF1 cDNA under the control of a heat-shock promoter. In HSN TM3, Sb/TM6 (gift from Leo Pallanck; Pallanck *et al.*, 1995a), HSN is carried on the third chromosome in association with TM3, Sb. A 37°C incubation drives the expression of dNSF1. The rescue of the *comt 17* phenotype was performed by crossing female *comt 17*/*comt 17*; +/+; +/+ flies to male +/Y; +/+; HSN TM3,Sb/TM6. Male *tubby* (associated with TM6) larvae (*comt 17*/Y; +/+; TM6/+) have the *comt 17* genotype but do not have the HSN rescue construct, whereas male non *tubby* (HSN,TM3, sb) larvae (*comt 17*/Y; +/+; HSN TM3, Sb/+) do.

Experiments with the use of these larvae were carried out in one of two ways as follows: WT and *comt 17* mid-third-instar larvae were selected and held in food vials containing 1 mM ecdysone for 1 h at 22°C followed by 2 h at 37°C in a water bath. Their leg and wing discs were dissected, fixed, and processed for conventional electron microscopy (EM) (see below). Alternatively, WT, *comt 17*, *comt 17*/Y; +/+; TM6/+, *comt 17*/Y; +/+; HSN TM3, Sb/+, mid-third-instar larvae were semidissected and incubated in vitro (see below) in the presence of 3 $\mu$M ecdysone at 37°C for 2 h. Their discs were removed, fixed, and processed for conventional EM (see below).

The stock "919" yw; P[w+, UAS-Fringe (DXD)-myc] was a gift from Matthew Freeman (Cambridge, United Kingdom). These flies carry the transgene comprising the Fringe cDNA in which the glycosyltransferase motif DDD motif has been replaced by a DXD that abolishes the glycosyltransferase activity but retains the Golgi localization (Munro and Freeman, 2000). Female flies were crossed to HsGAL4/Bc, El, Gla. We used Bc (Black Cell) as a larval marker. Two heat-shock treatments (each of 20 min at 37°C) were performed before larval collection. Mid-third-instar non Bc (UAS-Fringe-DXD-myc/HsGAL4) larvae were collected, their leg and wing discs dissected, and processed for immunofluorescence or immunoelectron microscopy (see below).

$ecd^{1ts}$ mutants ($ecd^{1ts}$ st ca) were a gift from Jean Antoine Lepesant (Paris, France). They are thermosensitive homozygote alleles that only produce a basal level of ecdysone at the restrictive temperature of 29°C (Garen *et al.*, 1977, Redfern and Bownes, 1983). Eggs were laid for 24 h and larvae grown for 6 d at 22°C (until second-instar/early third-instar larval stage). The vials were transferred at 29°C for 7 h. The larvae were then kept at 29°C or transferred back at 22°C for 18 h. Their discs were fixed for conventional EM.

Alternatively, after 7 h at 29°C, the discs were dissected and incubated in vitro in M3 medium (see below) in the absence or the presence of 3 $\mu$M ecdysone, omitting the fly extract in both cases. Their discs were fixed for conventional EM.

### *Conventional EM*

Early, mid-, and late third-instar larvae and white pupae were semidissected (disks, still attached to the head and the cuticle) and fixed for 2 h in 1% glutaraldehyde in 0.2 M phosphate buffer (pH 7.4) at room temperature and rinsed three to four times in 0.1 M cacodylate buffer (pH 7.4). Leg and wing imaginal discs were dissected further to remove any other tissues and processed for conventional EM as described in Rabouille *et al.* (1995b). Sections (50–60 nm) were cut on a Leica ultramicrotome, stained with uranylacetate and lead citrate, and were viewed under a Philips biotwin electron microscope.

### *Immunoelectron Microscopy*

Leg and wing discs were semidissected out of Fringe-DXD-myc-induced mid third-instar larvae (see above), fixed in 2% paraformaldehyde and 0.2% glutaraldehyde in 0.2 M phosphate buffer (pH 7.4) for 3 h at room temperature, and embedded in unicryl (British Biocell, Cardiff, United Kingdom) according to the standard protocol suggested by the company. Sections (50–60 nm) were cut on a Leica S4 and single labeled with 9E10 (mouse), MLO7 (rabbit), NN7 (rabbit) in 0.5% Fish skin gelatin in phosphate-buffered saline (PBS) followed by anti-rabbit IgG conjugated to 10-nm gold or anti-mouse IgG conjugated to 15-nm gold when appropriate. Sections were stained with lead citrate (5 min), 4% aqueous uranylacetate (40 min), and lead citrate (10 min) and were viewed under a Philips biotwin electron microscope.

### *Indirect Immunofluorescence*

Leg and wing discs were semidissected out of mid third-instar WT larvae and fixed at room temperature for 20 min in 3% paraformaldehyde in 0.2 M phosphate buffer (pH 7.4) supplemented with 0.1% Triton, followed by three to four times rinsing in PBS and storage at

4°C if necessary. The immunofluorescence procedure was as described previously (Rabouille *et al.*, 1999). Briefly, discs were incubated at room temperature for 30 min in PBS supplemented with 0.1% Triton and 0.225% fish skin gelatin (PBSTG), 3 h with the primary antibodies diluted in the same buffer, rinsed three times >1 h with PBSTG and 2 h with secondary antibodies conjugated with fluorescein isothiocyanate (FITC) or Texas Red in the dark, rinsed three times >30 min in PBSTG, and stored overnight in PBS. The discs were finely dissected and mounted in Vectashield containing 4,6-diamidino-2-phenylindole (DAPI). They were viewed under a Leica confocal microscope. The pictures were processed in Adobe Photoshop.

## Western Blotting

Leg and wings discs (30–50) were dissected from mid-third-instar WT larvae and homogenized directly in 100 μl of 1× SDS sample buffer (SSB) containing 5 mM dithiothreitol with the use of a motorized pestle. In one instance, 20 larval semidissected heads (including discs, brain, salivary glands, and cuticle) were homogenized in the same way.

The Kc cells were grown at 27°C in 10-cm Petri dishes containing 15 ml of M3 medium supplemented with heat-inactivated fetal bovine serum. They were harvested, spun, rinsed, and homogenized in 200 μl of buffer A (20 mM Tris-HCl, 1 mM EDTA, 10 mM $MgCl_2$, 10 mM KCl, 1 mM dithiothreitol, 0.23 M sucrose, and 1% Triton X-100). SSB was added to 1× final.

In the experiment with the use of *ecd*$^{1ts}$ mutant, the larvae were maintained for 7 h at 29°C, the discs were dissected and incubated in vitro in M3 medium (see below) in the absence or the presence of 3 μM ecdysone, omitting the fly extract in both cases. Thirty leg and 10 wing discs were finely dissected after each incubation (plus and minus ecdysone) and homogenized in 100 μl of 1× SSB. Protein (30 μg) was loaded on the gel. They were processed further with the use of affinity-purified MLO7 (anti-GM130 antibody) and the anti-β-tubulin antibody.

The same experiment was performed with the use of WT mid-third-instar larvae that were incubated in the presence or the absence of ecdysone in M3 medium (see below). Forty leg and 10 wing discs were finely dissected after each incubation (plus or minus ecdysone) and homogenized in 100 μl of 1× SSB. Protein (30 μg) was loaded on the gel. They were processed further for Western blotting as described below with the use of the antibody anti-sec23p (gift from Jean Pierre Paccaud, Geneva, Switzerland).

Western blotting was performed as described in Hui *et al.* (1997). The rabbit anti-GM130 antiserum and affinity-purified MLO7, and the rabbit anti-p115 antiserum NN7 were detected with the use of anti-rabbit IgG coupled to horseradish peroxidase. The mouse monoclonal anti-protein disulfide isomerase (PDI) antibody and anti-β-tubulin were detected with the use of anti-mouse IgG coupled to horseradish peroxidase. The enhanced chemiluminescence (Amersham Pharmacia Biotech, Buckinghamshire, United Kingdom) system was used to visualize the bands. The prestained molecular weight markers were purchased from Bio-Rad (Richmond, CA). The intensity of the bands was estimated with the use of NIH Image, version 1.62.

## In Vitro Disc Incubation

Leg and wing discs from mid-third-instar larvae of various genetic backgrounds were semidissected (still attached to the head and the cuticle) and incubated in a 3-cm plastic Petri dish for 10–18 h at 25°C in the Schneider or M3 medium (1.4 ml) supplemented by 5% hemolymph (fly extract made according to Currie *et al.* [1988] and 3 μM ecdysone (Sigma, Dorset, Poole, United Kingdom; from a 1 mM stock 10% ethanol) as described previously in Mandaron (1971). At the end of the incubation, the discs were fixed as described above for conventional electron microscopy or processed for Western blotting.

## Quantitation

***EM*** The Golgi area was defined by the Golgi stacked cisternae and immediate surrounding vesicles and tubules. Larval clusters were defined as the gathering of vesicles and tubules and cisternal profiles. To be counted as a larval cluster, at least four vesicles or tubules needed to be present and should not be >100 nm apart. In 85% of the cases the larval clusters occupied a specific location as being nested in a cup-shaped endoplasmic reticulum (ER) cisternae. Vesicles were defined as having an axial ratio of 1:1.5. Most were 50–70 nm in diameter but some were 2–3 times larger. A tubule was defined as having an axial ratio of at least 2:1 with a width of 70 nm. A cisterna has a width equal or <30 nm and was at least 200 nm in length. However, when dilated rims were linked to cisternal elements, they were considered as part of the cisternae. A cisternal stack is a profile where at least two cisternae overlap by at least 50% of their length. The cytoplasm was defined as the volume enclosed by the plasma membrane and excluding the nucleus (but including all other organelles).

Because one of the objective of this study was to define the relationship between the larval clusters and Golgi stacks, we chose the nonbiased name of organelle (org) to refer to either and both. In some instance, the org will be identifiable as Golgi area and in others, it will refer to larval clusters. The boundaries of the org were defined by the interface between the outmost membrane profiles and either the more amorphous cytoplasm or the cup-shaped ER cisternal membrane when present.

The surface density of the org within the cytoplasm ($S_{org}/V_{cyt}$) is the product of two distinct measurements: the surface density of the "organelle membrane" within the volume they occupy ($S_{org}/V_{org}$) multiplied by the volume density of the org within the cytoplasm ($V_{org}/V_{cyt}$).

Sorg/Vorg was estimated as follows: The boundary of the organelle (pictured at a magnification of 90 K) as well as all membrane within this boundary were marked. $S_{org}$ was estimated with the use of the intersection method by counting the number of intersections (ΣI) between the lines of a 3-mm grid and all the membrane comprised within the organelle boundary. $V_{org}$ was defined by the point hit method in counting the number of point hits falling within the boundary (ΣP) with the use of a 3-mm point grid. $S_{org}/V_{org}$ was $\Sigma I/\Sigma P \times mag$ ($\mu m^{-1}$) (Rabouille, 1999). Vcyt was estimated by point hit method with the use of pictures of cells at a magnification of about 10 K and a point grid. Results are expressed ±SD.

To estimate the percentage of membrane in cisternae, tubules, or vesicles, we used a series of vertical lines spaced by 5-mm overlapping pictures at ~90 K. Each intersection between the lines and each category of profile was scored and percentage estimated (Rabouille *et al.*, 1995b). The ratio of stacked cisternae on total cisternae was determined by the same method taking only into account the cisternal profiles.

***Immuno-EM.*** Pictures (10–20) were taken and printed at a magnification of 73 K. The relative distribution of gold particles over the ER and the organelle (either the larval clusters or the Golgi stacks when present) was established by counting the number of gold particles falling within the organelle boundary (see above) or on ER cisternae (plus nuclear envelope). One hundred percent represents the total number of gold falling on both compartments. The gold labeling corresponding to Fringe-DXD-myc was low and all gold particles summed, a method that does not give a SD. With the use of the point hit method (5-mm point grid), the nuclear background and the labeling density over the organelle was estimated (Rabouille, 1999).

***Immunofluorescence.*** Discs from WT early and late third-instar larvae were processed for immunofluorescence with the use of the anti-GM130 antibody (see above) and the average expression was estimated with the use of NIH Image, version 1.62. All the immunofluorescence pictures used for quantitative purposes were taken

at the same settings with the 20 or 40× objectives. The raw pictures were saved as black and white and were inverted. Boxes of different sizes were used to measure the intensity of fluorescence on the discs and on the surrounding area to estimate the background. Measurements (10–15) were performed on at least three pictures from three experiments.

## RESULTS

Our morphological studies focused on the leg and wing imaginal discs of third-instar larvae before, at, and after the onset of disc elongation. Discs from early and mid-third-instar larvae have not begun to elongate (average leg disc thickness 30–40 $\mu$m), whereas those from late third-instar larvae have (average thickness between 45 and 90 $\mu$m), and those from white pupae have completed the first phase of elongation (thickness ~240 ± 10 $\mu$m).

Discs were dissected from larvae at each developmental stage, fixed, and processed for conventional electron microscopy. We examined the surface section of the disc cells in each developmental stage (giving indication on the cell size) as well as the volume density of their cytoplasm (a measure of the cell volume occupied by the cytoplasm). Disc cells of the mid- and late third-instar larvae and white pupae were on average of the same size (our unpublished results) and 30% larger than the ones of early third-instar larvae represented largely by an increase in their cytoplasm. This indicates that the increase in disc thickness (600% increase) could be accounted for by the unfolding of the concentric folds (see INTRODUCTION) and was not accompanied by a substantial change in cell size except for the initial increase.

When observed at higher magnification, the cells of early third-larval instar discs appeared dense and their endomembranes poorly developed. These were interphase cells but we could not observe stacked Golgi cisternae. Instead, small clusters of vesicles and tubules (Figure 1, A and B) were observed often nested in the concavity of a cup-shaped ER cisterna. In many cases, this ER cisterna would define half to one-third of the boundaries of the clusters. The vesicles had a 50–70-nm diameter although larger profiles were also observed and the tubules were short (150–200 nm in length). The surface density of these clusters (Sorg/Vcyt) was 1.30 ± 0.07 $\mu m^{-1}$ (Table 1, line 1). The percentage of cluster membranes in vesicles, tubules, and cisternae was also established (Table 1, line 1). These small larval clusters consisted mostly of small vesicles (~82.5%) and tubules (~17.5%) but were almost devoid of cisternae (1%).

The cells of mid third-larval instar discs were less dense and we observed, again nested in ER cup-shaped cisternae in 85% of the cases, two kinds of profiles whose characteristics were reminiscent of those observed in the previous stage (Table 1, lines 3 and 4). First, small clusters (Sorg/Vcyt of 1.12 $\mu m^{-1}$) mostly contained vesicles and tubules (Table 1, line 3) with only 2.8% of the clusters membrane in cisternae, almost indistinguishable from the clusters observed in the early third-instar larvae; second, medium clusters (with a Sorg/Vcyt ~1.91 $\mu m^{-1}$) (Figure 1C) contained vesicles and tubules but with 12% of the membrane in cisternal elements (Table 1, line 4).

In late third-instar larvae, large clusters (with a Sorg/Vcyt ~3.17 $\mu m^{-1}$) contained 28.6% of their membrane in cisternae (Figure 1D) (Table 1, line 5). The largest of the clusters did exhibit stacked cisternae profiles. The remainder of membrane was observed as vesicles and tubules (Table 1, line 5).

Last, white pupal disc cells were examined and Golgi stacks were clearly visible. Their surface density within the cytoplasm was large (4.87 $\mu m^{-1}$; Table 1, line 6) and they comprised stacked cisternae (Figure 1E) and large tubular networks around cisternae (Figure 1F). The percentage of Golgi membrane found in cisternae rose to ~56.8%, of which 65% were stacked (Table 1, line 6).

This succession of different morphologies, from vesicles and tubules in larval clusters with increasing cisternal elements, to proper prepupal Golgi stacks, suggested a temporal conversion of vesicles and tubules to cisternae. However, the surface density of the organelle (that refers to larval clusters or Golgi stacks) within the cytoplasm (Sorg/Vcyt) increased as the cisternae formed. The surface density of organelle within the cytoplasm is composed of two components (see MATERIALS AND METHODS): First, the surface density of organelle membranes within the volume they occupy (Sorg/Vorg) measures how packed the membranes are within a unit of volume and was found similar from one stage to the next (Table 1, first numerical column); second, the volume density of the organelle membranes within the cytoplasm (Vorg/Vcyt) measures the cytoplasmic fraction occupied by these membranes within the cytoplasm and was found to increase from one stage to the next (Table 1, second numerical column). This means that the amount of membrane per unit of volume was similar at the different stages but that more membrane structures were added to the organelle, leading to an increase in the volume they occupy. Because of this addition of membrane, it is possible that the stacks we observed were not derived from the larval clusters but from entirely newly generated membranes. It is thus important to establish that the larval clusters are Golgi stack precursors.

### Drosophila *Golgi Markers and Antibodies*

We first addressed the question of the nature of the larval cluster membrane by localizing different Golgi proteins.

The rabbit polyclonal MLO7 antibody (gift from M. Lowe, Manchester, United Kingdom) was raised against the first 73 amino acids of human GM130 (Nakamura *et al.*, 1995; Lowe *et al.*, 1998), a Golgi peripheral membrane protein receptor for p115 (Nakamura *et al.*, 1997, see below). The corresponding 73 amino acids in the predicted *Drosophila* homolog of GM130 (AJ276417, CG11061) are 40% identical and 51% similar to human and rat GM130 with a very strong conservation in the first 25 (up to 64% identity and 84% similarity). The full-length dGM130 showed only 21% identity and 39% similarity to rat GM130 but exhibits the same overall coil-coiled structure (our unpublished results) and a similar richness in basic amino acids (such as glutamine 11.8 vs. 12.1% in rat GM130). dGM130 was mapped to 58 B7-C6 by probing a P1 array with the EST LP03286 (our unpublished results). By Western blotting with the use of either the antiserum or the affinity-purified MLO7 antibody, one strong band was revealed just above the 83-kDa marker (Figure 2A), which is slightly above the predicted molecular weight of dGM130 (790 amino acids). The same unique band was also revealed with the use of Kc cells (*Drosophila* derived tissue culture cell line) (Figure 2A).

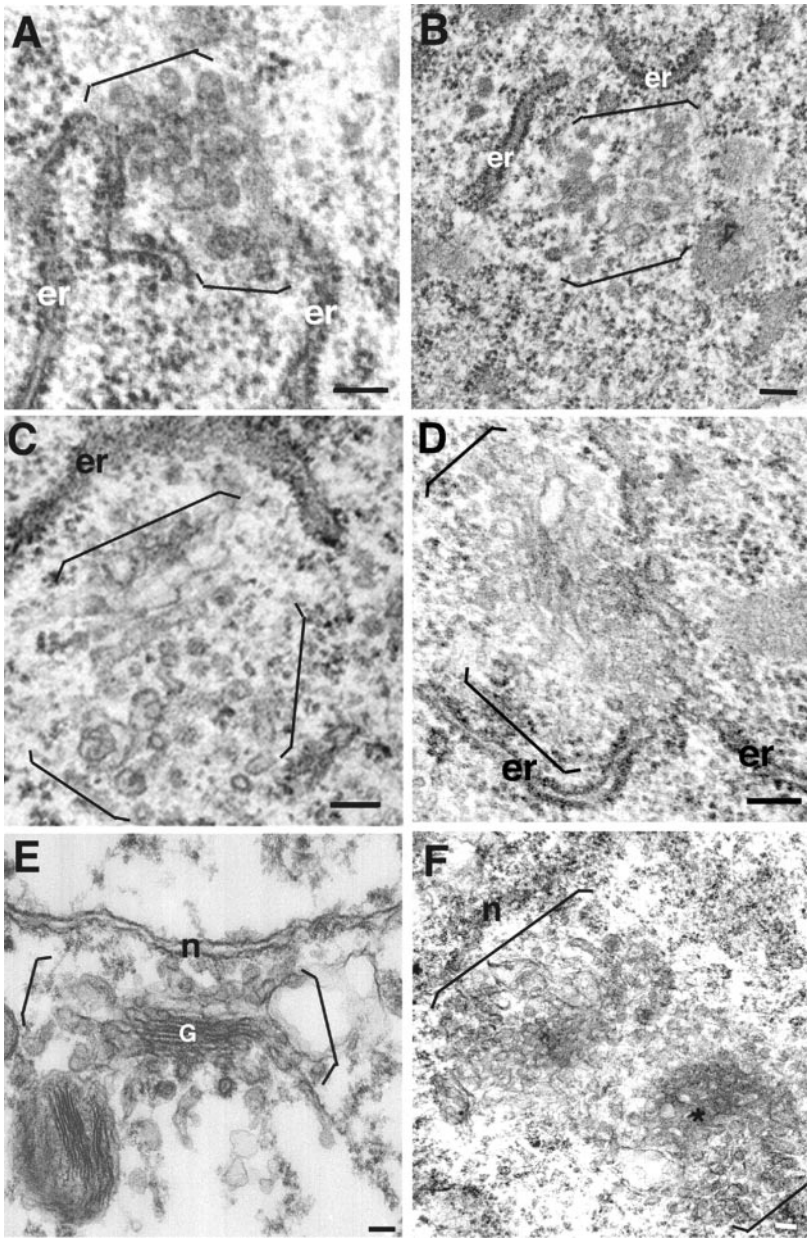


**Figure 1.** Larval clusters and Golgi areas in discs from third-instar larvae and white pupae. Larval clusters and Golgi area were visualized in leg and wing discs of early third-instar larvae (A and B), mid third-instar larvae (C), late third-instar larvae (D), and white pupae (E and F). Brackets mark the borders of the larval clusters and Golgi areas not bounded by ER cisternae. Stacks are marked with a G. In F, the asterisks indicate an en face view of a fenestrated cisternae. Note the proximity of the larval clusters to ER cisternae (er) in A–D. n, nuclear envelope. Bars, 100 nm.

The rabbit antiserum to p115 (NN7, gift from M. Lowe) was made against the full-length rat p115 protein (Nakamura *et al.*, 1997), a cytosolic myosin-like ligand for GM130. We cloned the *Drosophila* homolog of rat p115 (AJ272048, CG1422) by screening a *Drosophila* embryonic cDNA library (gift from Dr N. White, Edinburgh, United Kingdom) with the use of EST LD41079. A P1 clone array was also probed and dp115 was mapped to 7C6-8. dp115 is 50% identical and 67% similar to rat p115 with the same overall coil-coiled structure (our unpublished results) although the acidic tail (Dirac-Svejstrup *et al.*, 2000) is missing in dp115. When disc extracts were Western blotted with NN7 after electrophoretic separation, one band was observed at the 83-kDa molecular weight marker (Figure 2B), as expected (837 amino acids). The same band was reproduced with the use of another monoclonal antibody (mAb) against p115, 4H1 (our unpublished results).

The mouse monoclonal 1D3 antibody (1D3, gift from D. Vaux, Oxford, United Kingdom) was raised against the synthetic peptide corresponding to the 12 C terminus amino acids KDDDQKAVKDEL of human PDI that is a resident of the endoplasmic reticulum (Vaux *et al.*, 1990). In the *Drosophila* homolog of PDI (P543991, CG6988), this sequence becomes EEEEEAPKKDEL exhibiting ~60% similarity (McKay *et al.*, 1995). Used in a Western blot on a disc extract, 1D3 revealed one strong band around 50 kDa that corresponds to the predicted molecular weight of *Drosophila* PDI (496 amino acids; Figure 2B).

**Table 1.** Stereological analysis of the organelle (larval clusters and Golgi areas) at the different stages of disc elongation org refers to the larval clusters or the Golgi apparatus when clearly identifiable. Results are expressed as ±SD.

| | % of org membrane in | | | | | | |
|---|---|---|---|---|---|---|---|
| | $S_{org}/V_{org}$* in $\mu m^{-1}$ | $V_{org}/V_{cyt}$* | $S_{org}/V_{cyt}$* in $\mu m^{-1}$ | Vesicular profiles (%) | Tubules (%) | Total cisternae (%) | Stacked cisternae/total cisternae |
| Early third-instar larvae | 72.46 ± 8.1 | 0.018 ± 0.006 | 1.30 ± 0.07 | 82.5 ± 12.3 | 17.5 ± 12 | 1.0 ± 1.0 | nd |
| Mid-third-instar larvae | | | | | | | |
| Small clusters | 72.35 ± 5.4 | 0.0155 ± 0.003 | 1.12 ± 0.03 | 77.2 ± 8.4 | 20.0 ± 9.3 | 2.8 ± 2.0 | nd |
| Medium clusters | 68.28 ± 3.8 | 0.028 ± 0.004 | 1.91 ± 0.05 | 35.4 ± 15 | 49.1 ± 18 | 12.0 ± 5.0 | nd |
| Late third-instar larvae | 66.14 ± 2.7 | 0.048 ± 0.015 | 3.17 ± 0.09 | 28.4 ± 12.3 | 43.1 ± 10.1 | 28.6 ± 10.2 | 0.25 ± 0.10 |
| White pupae | 61.25 ± 6.4 | 0.079 ± 0.021 | 4.87 ± 1.1 | 12.8 ± 5.4 | 30.3 ± 12.3 | 56.8 ± 13.2 | 0.65 ± 0.20 |

nd, not determined.

* See MATERIALS AND METHODS for details.

The rabbit anti-Sec23p antibody (gift from J.P Paccaud, Geneva, Switzerland) was raised against a human sec23A peptide (Paccaud *et al.*, 1996) that shares 69% identity and 81% similarity with the predicted *Drosophila* Sec23p (AJ276482, CG1250). Sec23 is the sar1-specific GTPase activating protein (Yoshihisa *et al.*, 1993) and is part of the coat protein complex (COP) II machinery (Barlowe *et al.*, 1994). This antibody recognizes a single band in a disc extract at the predicted molecular weight of 77 kDa (Figure 10).

The rabbit anti-Sec31p antibody (gift from F. Gorelick, West Haven, NJ ) was raised against a rat Sec31 (Shugrue *et al.*, 1999). Rat Sec31 shares 33% identity and 51% similarity with *Drosophila* Sec31 (CG8266). Sec31 has been shown to be part of the COPII recruitment machinery (Schekman and Orci, 1996). This antibody recognizes a single band in a fly head extract that runs at a molecular weight consistent with a protein of 1264 amino acids (Figure 2B).

The anti-β-tubulin antibody (Sigma) and was raised against sea urchin sperm β-tubulin that shares 85% identity with the *Drosophila* counterpart. After Western blotting of disc extracts (Figure 10, C and D) and Kc cells extract (Figure 2A), one strong band was observed at the predicted molecular weight (503 amino acids).

The anti-δ-AP3 antibody (gift from M. Robinson, Cambridge, United Kingdom) was raised against the rat δ subunit of the AP3 complex that has high homology to the *garnet* gene product in *Drosophila*. δ-AP3 has been shown to localize in the *trans*-Golgi network in mammalian cultured cells (Simpson *et al.*, 1997) and in the Golgi area in S2 cells (Rabouille *et al.*, 1999).

The monoclonal mouse ascite 9E10 (gift from T. Nillson, Heidelberg, Germany) was used to detected the myc epitope (Nilsson *et al.*, 1993).

### *Larval Clusters Contain Golgi Proteins*

MLO7 was first used in indirect immunofluorescence experiments on WT mid-third-instar larvae. A punctate staining throughout the cytoplasm (Figure 3A), characteristic of the Golgi apparatus in *Drosophila* tissues was observed (Ripoche *et al.*, 1994; Stanley *et al.*, 1997; Rabouille *et al.*, 1999; Lecuit and Wieschaus, 2000; Munro and Freeman, 2000; Sisson *et al.*, 2000). This pattern is different from mammalian cells and is more reminiscent of a plant or yeast Golgi pattern (Rabouille *et al.*, 1999). In an effort to show the spatial arrangement of dGM130 staining with respect to other subcellular compartments in these very small disc cells (~5 μm across), the ER, the microtubules, and the nucleus were labeled with the use of the 1D3, the anti-β-tubulin antibody, and DAPI, respectively. The 1D3 pattern corresponded to the ER. It was found surrounding the nucleus and was also punctate (Figure 3B), but the dots were smaller, more numerous, and more scattered than the dGM130 pattern. The same pattern was visualized with the use of CEL5C (gift from Carol Lyons, Dundee, United Kingdom), a mAb raised against human ribophorin I, a resident of the ER (our unpublished results).

When 1D3 was used in a double labeling experiment with MLO7, it revealed that dGM130 colocalized partially with the ER (Figure 3C) in agreement with our EM studies. A similar double-labeling pattern was observed when CEL5C was used instead of 1D3 (our unpublished results). A double labeling experiment with the use of β-tubulin antibody and MLO7 (Figure 3D) showed a different pattern. There was almost no overlap and no clear spatial relationship could be established. These results indicate that the dGM130 pattern was specific and exemplified the Golgi pattern. A very similar result was obtained with NN7 (an antibody to p115) (Figure 3E) and the anti-δ-AP3 antibody (Figure 3F).

The glycosyltransferase Fringe has recently been shown to be a Golgi protein (Bruckner *et al.*, 2000; Munro and Freeman, 2000). Transgenic flies carrying UAS-Fringe-DXD tagged with the myc epitope provided us with an alternative tool to confirm the Golgi nature of the disc larval clusters. Fringe localization in the fly Golgi apparatus was shown to be unaffected when the glycosyltransferase motif DDD was changed to DXD (Munro and Freeman, 2000). Fringe-DXD-myc was expressed ubiquitously at low level (see MATERIALS AND METHODS) and with the use of 9E10 (a monoclonal anti-myc antibody) on sections of unicryl-embedded discs, it was localized to larval clusters (Figure 4, A and B) and Golgi stacks (Figure 4C) when present (the heat shock necessary to induce Fringe expression has driven some of the clusters to be converted into stacks, see below; Figure 7B). The number of gold particles corresponding to Fringe

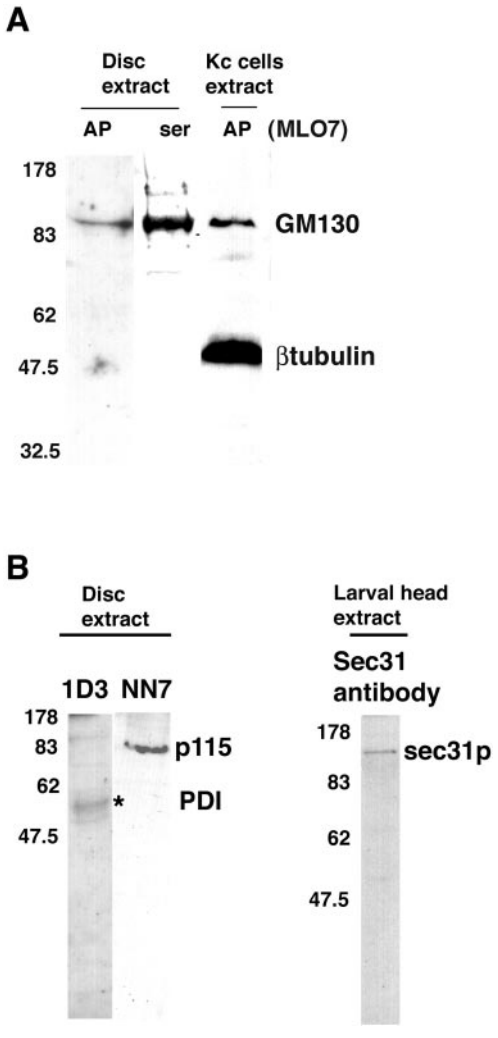


**Figure 2.** Western blot of *Drosophila* tissues and Kc cells. (A) Imaginal disc and Kc cell extracts were blotted with either the MLO7 serum (ser) or the MLO7 affinity-purified antibody (AP) raised against the 73 N-terminal amino acids of human GM130. One strong band just above the 83-kDa molecular weight marker is visible in all lanes. The Kc cell extract was also blotted with the anti-$\beta$-tubulin mAb and a band at 50 kDa is visible. Disc extract protein (45 $\mu$g, equivalent of 8–10 discs) and 100 $\mu$g of Kc cell extract protein were loaded on the 8% acrylamide gel. (B) Disc extract was blotted with 1D3. One band at 50 kDa (asterisk) was revealed in addition to two fainter bands just below and one above the 83-kDa marker. Disc extracts (45 $\mu$g) were also blotted with NN7 and one strong band was revealed at ~83 kDa. Disc extract protein (equivalent of 8–10 discs) was loaded on the 10% acrylamide gel. Larval head extract was blotted with an anti-Sec31p antibody. One band was revealed at ~130 kDa. Protein (40 $\mu$g) was loaded (equivalent to 5 heads) on a 6% acrylamide gel. The numbers on the left of the blots indicate the molecular weight of the prestained markers.

was low. We summed 65 gold particles in >20 pictures. The labeling was confined to the ER (35%) and larval clusters or Golgi stacks (65%). No other membrane compartment was labeled although we could see a low percentage of gold particles at the plasma membrane.

With the use of the same material, MLO7 was used to visualize dGM130 that was found in larval clusters (Figure 4, D and E) and stacks (Figure 4F). Again, the only membrane compartments that were labeled were the clusters or stacks (66.6 ± 12.8%) and the ER (33.4 ± 9.9%) (167 gold counted). This result was comparable to results obtained in WT mid-third-instar larvae (our unpublished results). A very similar result was obtained with NN7 visualizing dp115 (Figure 4, G-I). The clusters and stacks were labeled (67.1 ± 10.6%) as well as the ER (32.9 ± 8.6%) (147 gold counted). The labeling density over the stacks or the larval clusters was 9.8 ± 3.2 times over background for Fringe-DXD-myc, 10.1 ± 4.1 for dGM130, and 8.4 ± 2.9 for dp115. Similar results were also obtained with the *Drosophila* mannosidase II (our unpublished results).

Immunofluoresence imaging indicated that Fringe appeared localized in spots surrounding the nucleus (Figure 5A) in a similar manner to dGM130. Imaginal discs were labeled with MLO7 and 9E10, respectively. When the level of Fringe expression was low, the overlap with dGM130 was significant (Figure 5, B and C). 84 ± 5.7% of structures observed were either yellow (complete overlap) or were partially yellow in combination with either green or red or both. The same pattern was observed with NN7 (visualizing dp115) that also colocalized with Fringe-DXD-myc (Figure 5, D and E). 80 ± 7.6% of the structures observed were either partially or completely yellow. The lack of total overlap, we believe, is mostly due to the fact that the protein expression between clusters is not uniform even for endogenous proteins. We have found it technically difficult to visualize colocalization in situations where Fringe and either dGM130 or dp115 were expressed at very different levels. Taken together, these results suggest that the larval clusters contained at least three Golgi markers (dGM130, dp115, and Fringe), and therefore suggest that an unknown yet significant proportion of the membranes comprised within the larval clusters is Golgi membranes.

### *ER Exit Sites*

The larval clusters in early third-instar larvae consisted of >80% vesicles most of them being 50–70 nm in diameter, consistent with the geometrical features of COPI and II vesicles. Larval clusters were also very often (85% of the cases) found in proximity to a cup-shaped ER cisterna, which resembles an ER exit site (Oprins *et al.*, 1993; Orci *et al.*, 1994). Because COPII vesicles are known to bud from ER at the ER exit sites (Barlowe *et al.*, 1994, Martinez-Menarguez *et al.*, 1999), the vesicles comprised within the larval clusters could be COPII-derived vesicles. Sec23p and Sec31p are part of the COPII machinery (Schekman and Orci, 1996) and we used antibodies raised against these two proteins to label these sites. The immunofluorescence patterns of dSec23p and dSec31p were reminiscent of that of dGM130. They were punctate, surrounded the nucleus and only colocalized partially with the ER labeled with 1D3 (Figure 6, A and B) or CEL5C (our unpublished results).

Discs were also labeled for dSec23p, dSec31p, and Fringe-DXD-myc (Figure 6, C and D). When the level of Fringe expression was low, these markers exhibited ~60% colocalization, approaching the figures obtained with dGM130, dp115, and Fringe. These results suggest that dGM130,

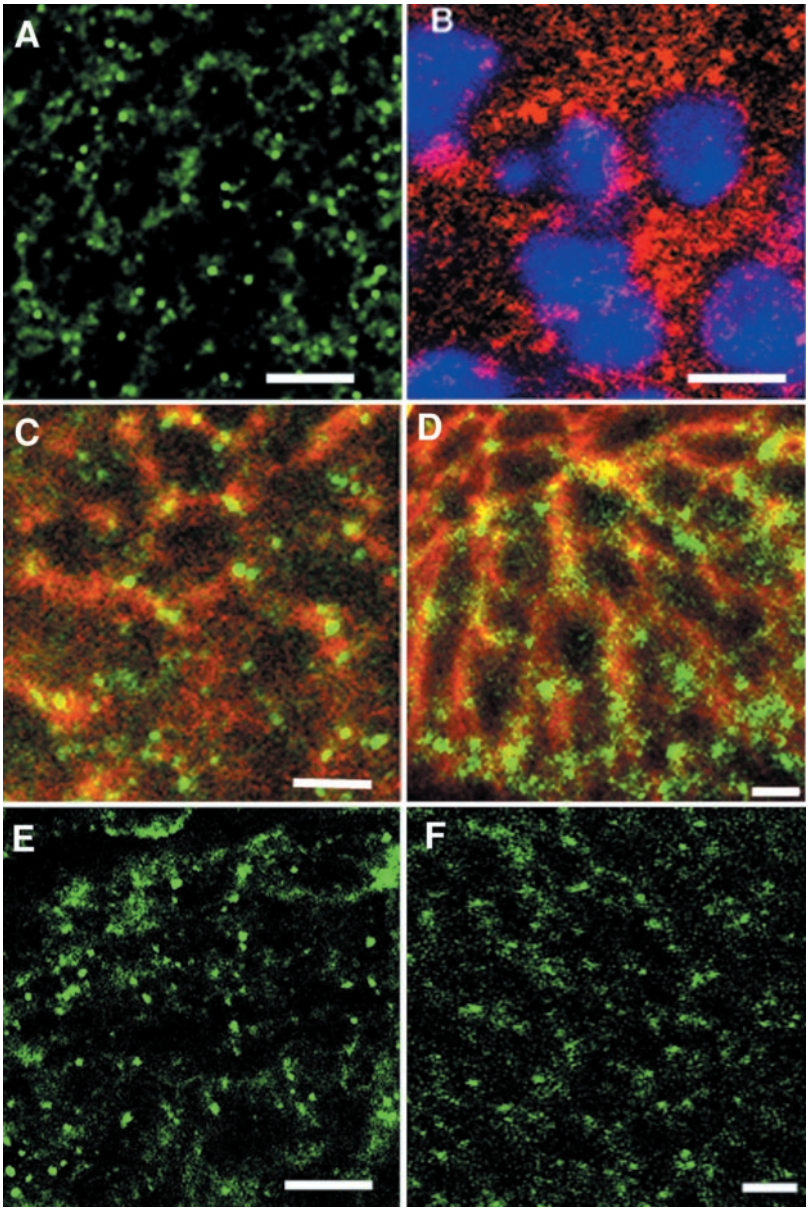


**Figure 3.** Immunofluorescence imaging of the larval clusters in imaginal disc cells. dGM130 immunofluorescence pattern was visualized in mid-third-instar larval leg and wing discs labeled with rabbit polyclonal MLO7 serum followed by an anti-rabbit IgG conjugated with FITC (green) (A). Note the dots surrounding a black space (nucleus). Discs were also labeled with mouse monoclonal 1D3 followed by an anti-mouse IgG conjugated with Texas Red (red), and DAPI (blue) (B). Dots are numerous and also surround the nucleus. Discs were double immunolabeled with the use of MLO7 and 1D3 followed by an anti-rabbit IgG conjugated with FITC (green) and an anti-mouse IgG conjugated with Texas Red (red) (C). Note that the green dots overlap partially with the red staining representing the ER. Discs were double immunolabeled with MLO7 and the mouse monoclonal anti-$\beta$-tubulin antibody followed by an anti-rabbit IgG conjugated with FITC (green) and an anti-mouse IgG conjugated with Texas Red (red) (D). Discs were also labeled with NN7 (the anti-p115 antibody) (E) and the anti-$\delta$-AP3 antibody (F) followed by a anti-rabbit IgG conjugated with FITC. Note that the pattern in A, E, and F are similar. Bars, 5 $\mu$m.

dp115, dSec23p, dSec31p, and Fringe-DXD-myc localize in the same structure (the larval clusters) and that they were populated by COPII-coated vesicles.

### *Larval Clusters Can Be Driven to Form Stacked Cisternae*

To support further the fact that the larval clusters are Golgi stack precursors, we attempted to force the conversion of these clusters into Golgi cisternae.

Mid-third-instar WT larvae were incubated at 37°C for 2 h. Under these conditions, the larvae were viable, and aged but did not become pupae. The larval clusters present in the larvae before the temperature shift consisted of tubules and vesicles with ~7% of the total membrane in cisternae and had a surface density of 1.91 $\mu m^{-1}$ (Table 2). When incubated at 22°C for 2 h (Figure 7A), the larval clusters have grown a little (surface density of 2.04 $\mu m^{-1}$), and have consisted of small tubules and vesicles with 10% of membrane in cisternae (Table 2). When incubated at 37°C, however, they were replaced by small stacks of cisternae (Figure 7B) with 45% of total Golgi membrane in cisternae (Table 2) with 45% of them in stacks. Importantly, the surface density of the clusters and the resulting cisternae were not grossly modified by the 37°C incubation (3.09 $\mu m^{-1}$ after incubation vs. 2.04 $\mu m^{-1}$ before, a 1.51-fold difference), whereas the gain in membrane in cisternae was 6.4-fold (from 7 to 45%) (Table 2). This result suggests that most of the membrane present in larval clusters before the incubation was converted into Golgi-stacked cisternae.

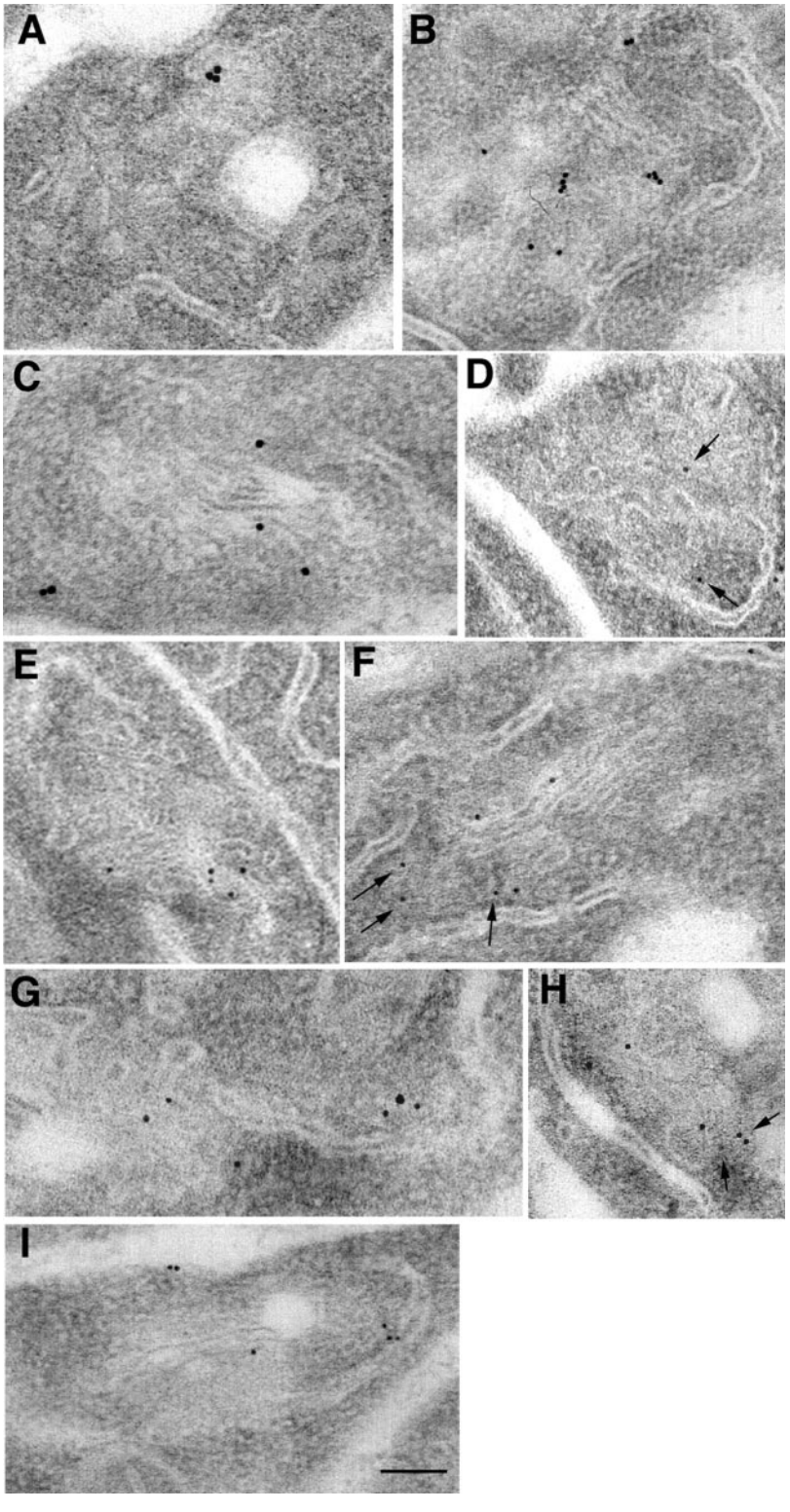


**Figure 4.** Immuno-EM localization of Golgi proteins on larval clusters and Golgi stacks. Unicryl-embedded mid-third-instar discs expressing low level of Fringe-DXD-myc were sectioned and labeled with 9E10 (anti-myc antibody) followed by anti-mouse IgG conjugated to 15-nm gold (A–C) MLO7 (anti-GM130 antibody) followed by anti-rabbit IgG conjugated to 10-nm gold (D–F), and NN7 (an anti-p115 antibody) followed by anti-rabbit IgG conjugated to 10-nm gold (G–I). Larval clusters (A, B, D, E, G, and H) and Golgi areas comprising a stack (C, F, and I) were labeled by the three antibodies. The arrows in D, F, and H indicate gold particles that may be difficult to see. Bar, 100 nm.

### *dNSF1 and Formation of Golgi Stacks*

The conversion of clusters of tubules and vesicles into cisternae would imply the fusion of the former fragments into the latter as observed in the reassembly of Golgi stacks in vitro (Rabouille *et al.*, 1995b). Two ATPases are known to be involved in the reassembly of Golgi fragments into stacked

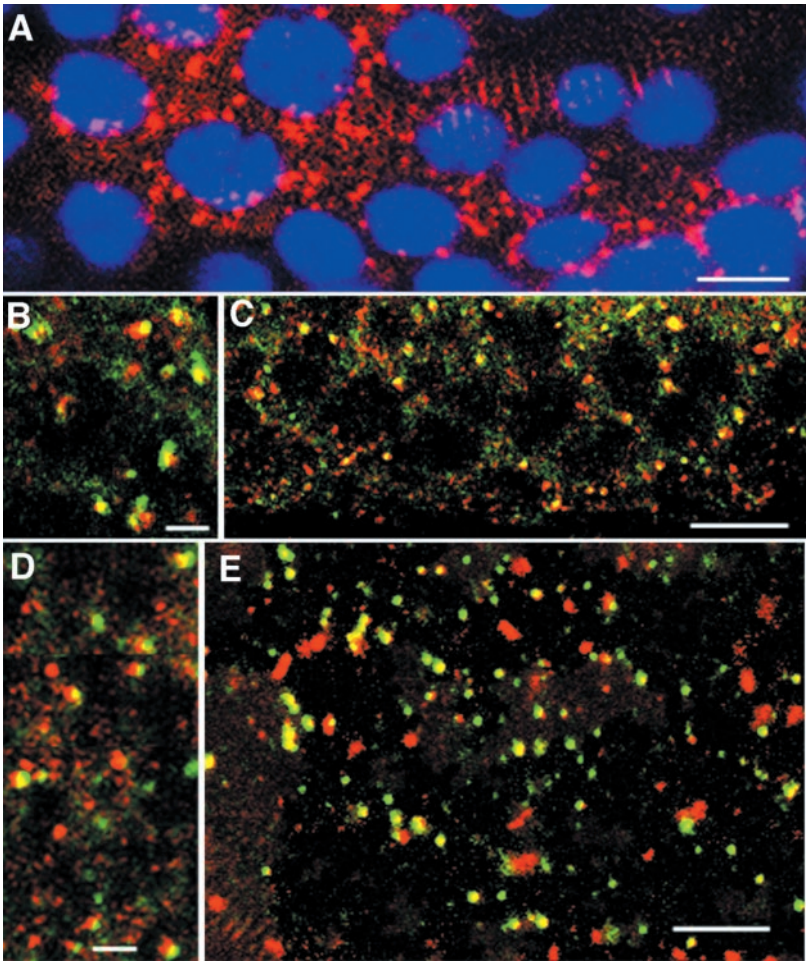


**Figure 5.** dGM130, dp115, and Fringe in mid-third-instar larval discs cells. UAS-Fringe-DXD-myc (stock 919)/HsGAL4 mid-third-instar larval discs were immunolabeled after heat shocking the larvae to induce the synthesis of myc-tagged Fringe-DXD. These discs were immunolabeled with the monoclonal anti-myc antibody 9E10 followed by an anti-mouse IgG conjugated with Texas Red (red), and DAPI (blue) (A). Note the dots around the nucleus. These discs were also double labeled with 9E10 and either MLO7 (B and C) or NN7 (D and E) followed by an anti-mouse IgG conjugated with Texas Red (red) and an anti-rabbit IgG conjugated with FITC (green). Note the colocalization of the two proteins (yellow) and also the structures that display all three colors (yellow, green, and red). Bars, 5 $\mu$m.

cisternae in vitro, NSF (and its cofactor $\alpha$SNAP), and p97 (and its cofactor p47) (Acharya *et al.*, 1995; Rabouille *et al.*, 1995a; Kondo *et al.*, 1997). We tested the involvement of dNSF1 (one of the two *Drosophila* homologs of mammalian NSF) in the observed Golgi stack biogenesis with the use of larvae from *comt 17* homozygote stocks (gifts from Dr. B. Ganetsky). *comt 17* is a thermosensitive allele of dNSF1. At 37°C, dNSF1 is misfolded and nonfunctional (Siddiqi and Benzer, 1976; Pallanck *et al.*, 1995a). We performed parallel experiments with WT larvae as well as with larvae in which the dNSF1 mutation (*comt 17*) is rescued by a dNSF1 transgene under the control of a heat-shock promoter (HSN) (see MATERIALS AND METHODS for details). Because the production of mutant dNSF1 and the overexpression of dNSF1 were both dependent on an incubation at 37°C, all experiments were performed concurrently under equivalent conditions.

In contrast to what happened in the WT situation (Figure 7B), the formation of Golgi cisternae in *comt 17* larval discs exposed to the same conditions as WT (37°C for 2 h, see above) was blocked. The larval clusters that were present in disc cells from *comt 17* larvae before the incubation remained as tubules and vesicles (Figure 7C) with only ~17% of the total Golgi membranes in cisternae (Table 2). Furthermore, ecdysone is known to trigger disc elongation and its production by the prothoracic gland depends on the neuropeptide prothoracicotropic hormone whose secretion ultimately might depend of dNSF1. Although exogenous ecdysone was fed to the larvae to prevent any effects of the lack of production of ecdysone in the NSF mutant larvae, we also performed the experiment in vitro in the presence of exogenous ecdysone (for details, see below and MATERIALS AND METHODS). *comt 17* larvae were dissected and their discs incubated at 37°C for 2 h in the presence of ecdysone. The same results were obtained as in vivo. The larval clusters did not become Golgi stacks (Figure 7D and Table 2). The conversion of larval clusters into Golgi stacks, however, was rescued by overexpression of dNSF1. In the *comt17*/Y; HSN TM3, sb/+ larvae, the conversion from larval clusters to Golgi stacks was even more efficient than in WT (53% of membrane in cisternae, of which 64% were in stacks; Table 2 and Figure 7F). The level of dNSF1 in these larvae was at least 3 times that of the WT larvae (as estimated by fluorescent in situ hydridization; our unpublished results) and that could explained why the rescue was more efficient than the WT. The *comt 17*/Y; TM6/+ larvae (nonrescued) were very similar to the homozygote *comt 17* larvae (Figure 7E and Table 2).

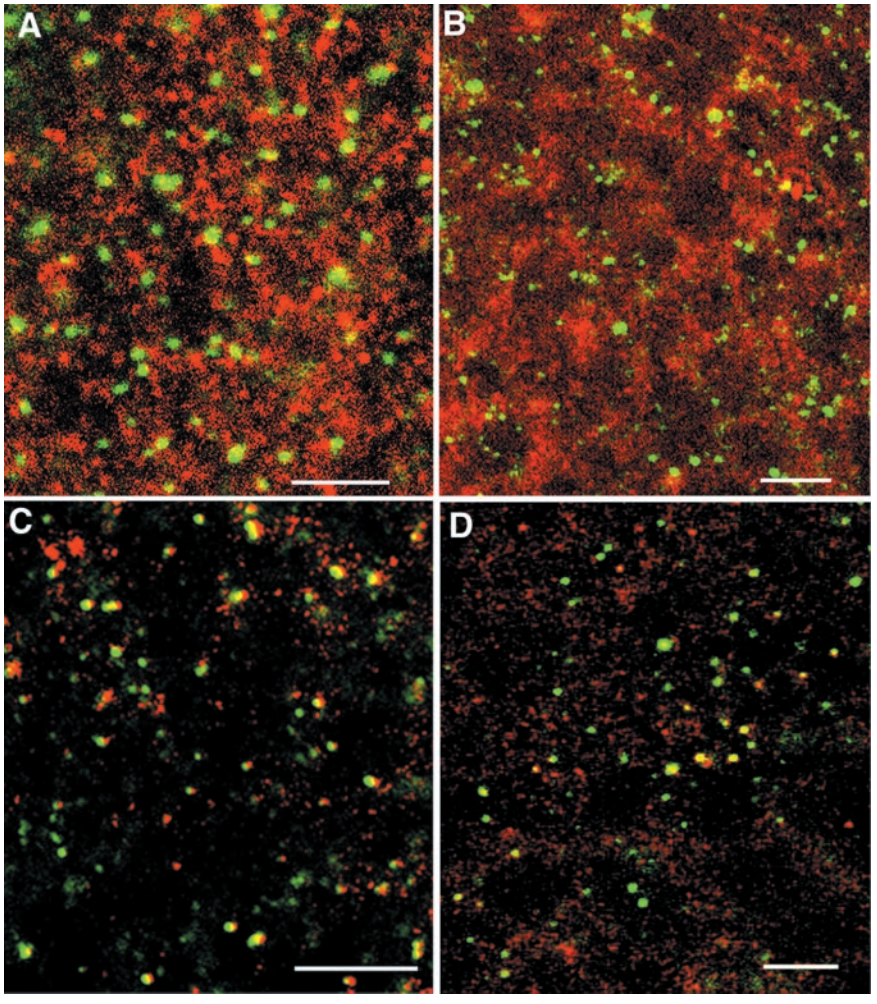


**Figure 6.** Immunofluorescence labeling of the larval clusters with components of the COPII machinery. UAS-Fringe-DXD-myc/HsGAL4 mid-third-instar larval discs (Fig .5) were immunolabeled with the anti-Sec23p antibody (A and C) or Sec31p antibody (B and D) together with 1D3 (A and B) and 9E10 (C and D) followed by an anti-rabbit IgG conjugated with FITC and an anti-mouse IgG conjugated to Texas Red. Note in C and D structures in which dSec23p, dSec31p, and Fringe overlap completely or partially together with structures that contain only dSec23p or dSec31p or only Fringe. Bars, 5 $\mu$m.

This series of experiments suggests that the larval clusters can be converted to stacked cisternae with only minimal addition of new membrane. This conversion was blocked in the absence of functional dNSF1 and was rescued by overexpression of functional dNSF1. Taken together, these results suggest the system we are studying could represent an in vivo system in which to study the biogenesis of Golgi stacks.

### *Biogenesis of Golgi Stacks Is Dependent on Ecdysone*

The timing of the transition from larval clusters to stacked cisternae was suggestive of an involvement of ecdysone, the hormone that plays a crucial role in the morphogenetic event of larval-to-pupal transition (Garen *et al.*, 1977).

We first recapitulated the transition from larval clusters to Golgi stacks in a semi-intact system (Mandaron, 1971) that reconstituted disc elongation in vitro with the use of dissected discs incubated in M3 medium containing exogenous ecdysone. A 10–18-h incubation was successful in mimicking the first step of disc elongation (our unpublished results). This incubation drove the conversion of clusters of vesicles and tubules to Golgi areas comprising 58.8% cisternae (Figure 8C and Table 3), similar to figures obtained in white pupae Golgi areas (Table 1, line 6). In the absence of ecdysone, this morphological change did not occur (Figure 8, A and B, and Table 3).

These results suggest that the coupling of disc elongation and the biogenesis of the Golgi stacks can be reconstituted in vitro and that the disc culture system mimics closely the in vivo situation. Moreover, they also suggest that ecdysone could be the trigger of Golgi stack biogenesis.

To investigate the latter, we then turned toward the *ecdysoneless* mutants $ecd^{1ts}$, a *Drosophila* temperature-sensitive allele. At the restrictive temperature of 29°C, ecdysone production is severely inhibited (Garen *et al.*, 1977; Redfern and Bownes, 1983), whereas at 22°C, the larvae behave as WT. Six days after egg laying at 22°C, the larvae were transferred to 29°C for 7 h. After maintaining the larvae at 29°C or returning them at 22°C for 18 h, the larvae were dissected and the discs processed for electron microscopy. When maintained at 29°C, the only profiles observed were clusters of vesicles and tubules (Figure 9A). The surface density (Sorg/Vcyt) was 2.86 $\mu m^{-1}$ and the percentage of mem-

**Table 2.** Effect of the *comt 17* mutation on the formation of Golgi stacks. org refers to the larval clusters or the Golgi when clearly identifiable. Results are expressed as ±SD.

| | | | % of org membrane in | | | |
|---|---|---|---|---|---|---|
| | | $S_{org}/V_{cyt}$* ($\mu m^{-1}$) | Vesicular profiles (%) | Tubules (%) | Total cisternae (%) | Stacked cisternae/total cisternae |
| WT | Before incubation | 1.91 ± 0.20 | 36.0 ± 8.6 | 57.1 ± 7.8 | 7.0 ± 3.5 | nd |
| | After 2-h incubation at 21°C in vivo | 2.04 ± 0.21 | 32.4 ± 9.3 | 42.5 ± 6.5 | 10.1 ± 3.9 | nd |
| | After 2-h incubation at 37°C in vivo | 3.09 ± 0.31 | 20.5 ± 4.9 | 34.1 ± 5.7 | 45.0 ± 8.2 | 0.45 ± 0.12 |
| *comt 17* | After 2-h incubation at 37°C in vivo | 3.64 ± 0.27 | 34.7 ± 6.8 | 49.3 ± 6.7 | 16.8 ± 9.7 | nd |
| | After 2-h incubation at 37°C in vitro | 3.65 ± 0.30 | 38.6 ± 5.9 | 45.8 ± 7.4 | 15.2 ± 8.6 | nd |
| *comt 17*/Y; TM6/+ | After 2-h incubation at 37°C in vitro | 4.13 ± 0.62 | 35.1 ± 6.8 | 50.1 ± 10.3 | 14.8 ± 7.3 | nd |
| *comt 17*/Y; HSN TM3, sb/+ | After 2-h incubation at 37°C in vitro | 6.99 ± 0.73 | 14.3 ± 7.5 | 32.7 ± 8.6 | 53.0 ± 5.4 | 0.64 ± 0.1 |

nd, not determined.

* See MATERIALS AND METHODS for details.

brane in cisternae was 7.0% (Table 3). When returned to 22°C for 18 h, the Golgi area was now neatly defined as stacked cisternae (Figure 9B). The surface density of the Golgi areas was not significantly different from the 29°C larvae (3.31 $\mu m^{-1}$; Table 3) but the percentage of membrane in cisternae was 60.9%, a highly significant increase, of which 72% in stacks (Table 4).

A similar experiment was performed in vitro. After maintaining the larvae at 29°C for 6 h, the larvae were dissected and incubated in M3 medium at 22°C in the presence or absence of ecdysone. Discs incubated without ecdysone exhibited larval clusters (Figure 9C) with a surface density of 3.24 $\mu m^{-1}$ and 4.6% of membrane in cisternae (Table 3), whereas the discs incubated in the presence of ecdysone presented stacked cisternae (Figure 9D) with surface density of 2.86 $\mu m^{-1}$ and 47.7% of membrane in cisternae (Table 3).

We took these results as additional evidence that the larval clusters were Golgi stack precursors. As in the in vivo experiment described above with WT larvae (Figure 7, A and B), the conversion of clustered vesicles and tubules to stacked cisternae was achieved without substantial addition of new membranes, possibly suggesting that Golgi stacks were built via consumption of the larval clusters. These results also suggest that ecdysone played an important role in the conversion of the larval clusters into Golgi stacks.

### *dGM130 and dSec23 Protein Expression Increases in Presence of Ecdysone*

Disc elongation does not take place in the absence of ecdysone. The blockade of Golgi stack biogenesis in the absence of ecdysone could therefore be a consequence of the blockade of disc elongation. Alternatively, Golgi stack biogenesis could be an event independently triggered by ecdysone.

To address part of this issue, we investigated whether ecdysone could have an effect on the expression of Golgi-related proteins. Leg and wing discs dissected from mid-and late third-instar larvae were processed for immunofluorescence with the use of MLO7, the anti-GM130 antiserum. In mid-third-instar larvae, the general expression of dGM130 was low (Figure 10A) with no detectable pattern as observed in Figures 3 and 5. In contrast, dGM130 expression elevated in late third-instar larvae (Figure 10B), approximately three- to fourfold on average (n = 4).

Furthermore, disc were collected from either $ecd^{1ts}$ mutant larvae maintained at 29°C or from WT mid-third-instar larvae and they were incubated in vitro in the presence or the absence of ecdysone. Western blotting of the $ecd^{1ts}$ disc extracts with MLO7 revealed that in the presence of ecdysone the band corresponding to dGM130 has an intensity approximately threefold higher than in the absence of ecdysone (n = 2; Figure 10C). Similar results were obtained by Western blotting of WT disc extracts with MLO7 or the anti-Sec23 antibody. In the presence of ecdysone, the band corresponding to dGM130 was 2.7 times more intense (n = 2; our unpublished results) and the band corresponding to dSec23p was approximately fivefold more intense than without ecdysone (Figure 10C) for a constant expression of β-tubulin. This experiment suggests that dGM130 and dSec23 protein expression is dependent on ecdysone and that ecdysone might trigger Golgi stack biogenesis.

## DISCUSSION

### *Golgi Stack Biogenesis In Vivo*

We have shown that Golgi stack biogenesis occurs in epithelial imaginal disc cells during the first phase of disc elongation in *D. melanogaster*. As larvae become white pupae, their leg and wing imaginal discs elongate, and the morphology of the Golgi apparatus within the disc cells changes. The morphological changes begin in early third-

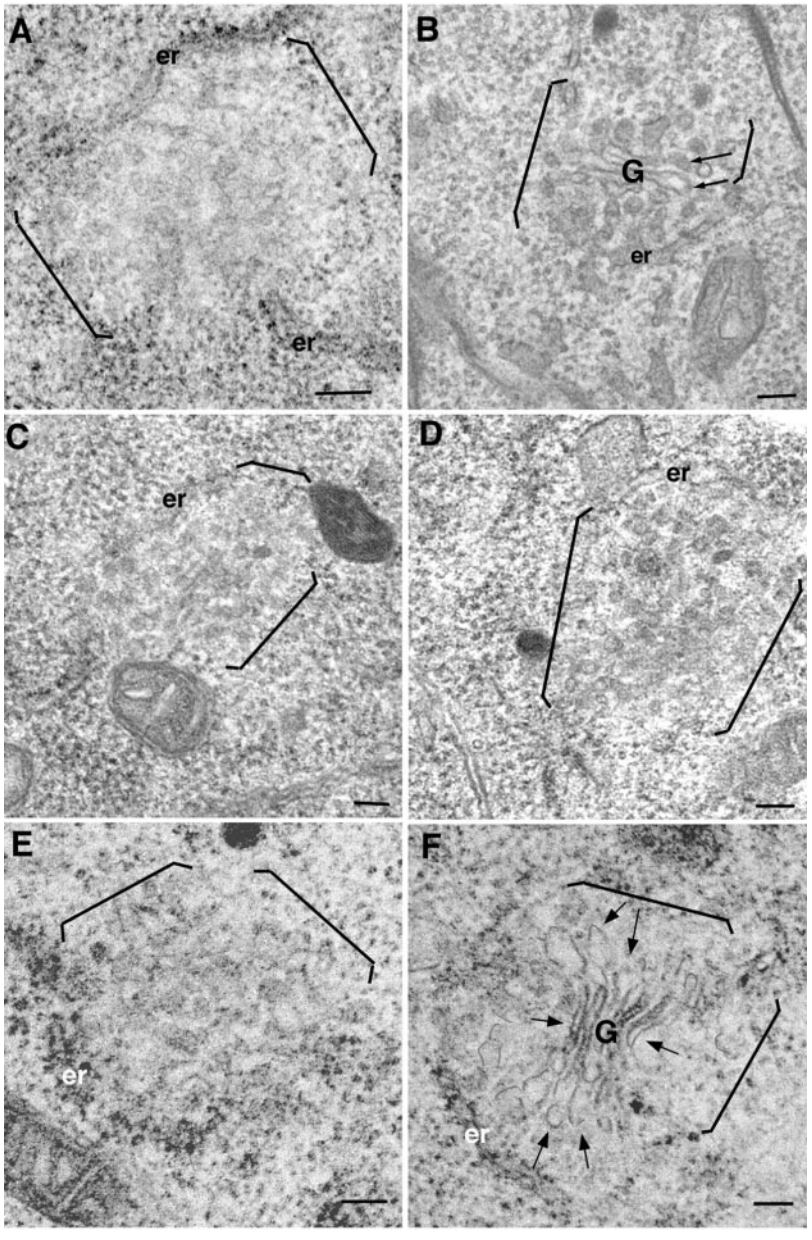


**Figure 7.** Effect of the *comt 17* mutation on the biogenesis of Golgi stacks. Mid-third-instar WT larvae were incubated at 22°C (A) or at 37°C (B) for 2 h. followed by dissection of their discs. *Comt17* homozygote larvae were incubated at 37°C for 2 h followed by disc dissection (C) or semidissected and incubated at 37°C for 2 h in the presence of ecdysone (D). *comt 17*/Y; TM6/+ (E) and *comt 17*/Y; TM3 HSN, Sb/+ (F) larvae were semidissected and incubated at 37°C for 2 h in the presence of ecdysone. The discs were fixed and processed for conventional EM. The larval clusters and the Golgi areas are marked between brackets when ER cisternae are not marking the natural boundaries, and the stack marked with a G. Note the cisternae in B and F (arrows). er, endoplasmic reticulum. Bars, 100 nm.

instar larvae with the presence of small larval clusters of 50–70-nm vesicles and short tubules. Through mid- to late third instar, these small clusters are gradually replaced by larger clusters of vesicles and longer tubules as well as some cisternal elements. There appears to be a correlation between the size of the clusters and the percentage of cluster membrane in cisternal profiles. And finally, in white pupae, the larval clusters are replaced by still larger Golgi-stacked cisternae of typical morphology. This succession of morphologies suggests that the small larval clusters increase in size with a concomitant formation of cisternae, up to ~60% of the Golgi membrane, of which two-thirds are in stacks.

The transition from small Golgi fragments to stacked cisternae appears to be a phenomenon not confined solely to *Drosophila* larval disc development. Rather, preliminary results suggest that the same transition occurred during *Drosophila* embryogenesis. In syntitial and gastrulating embryos, the Golgi apparatus consists of small fragments (Fullilove and Jacobson, 1971; Ripoche *et al.*, 1994; Stanley *et al.*, 1997), whereas in late embryo (20 h after fertilization), it has the typical stacked morphology (Rabouille *et al.*, 1999). A similar change in the Golgi morphology (from clusters to stacks) also occurs in *Drosophila* salivary glands (Thomopoulos *et al.*, 1992) between early and late-third-instar larvae, coinciding with glue synthesis. The apparent morphological changes could suggest that the morphological state of the Golgi apparatus are linked to the developmental state of the cell, even maybe to its commitment to differentiation.

**Table 3.** Stereological analysis of the effect of ecdysone on the formation of the Golgi stacks. org refers to the larval clusters or the Golgi are when clearly identifiable. Results are expressed as ±SD.

| | | | % of org membrane in | | | |
|---|---|---|---|---|---|---|
| | | $S_{org}/V_{cyt}$* ($\mu m^{-1}$) | Vesicular profiles | Tubules | Total cisternae | Stacked cisternae/ total cisternae |
| WT in vitro | −ecd | 2.04 ± 0.42 | 43.5 ± 16.6 | 44.0 ± 13.1 | 11.5 ± 5.0 | nd |
| | +ecd | 5.42 ± 1.13 | 13.8 ± 5.5 | 26.9 ± 7.9 | 58.8 ± 10.3 | 0.61 ± 0.10 |
| *Ecd*$^{1ts}$ in vivo | at 29°C | 2.86 ± 0.74 | 28.5 ± 9.7 | 65 ± 14 | 7.0 ± 3.6 | nd |
| | at 21°C | 3.31 ± 0.50 | 16.1 ± 5.6 | 23.1 ± 10 | 60.9 ± 15.0 | 0.72 ± 0.24 |
| *Ecd*$^{1ts}$ in vitro | −ecd | 3.24 ± 0.43 | 32.1 ± 10 | 63.0 ± 15 | 4.6 ± 4 | nd |
| | +ecd | 2.86 ± 0.20 | 22.6 ± 3.5 | 29.1 ± 8.2 | 47.7 ± 7 | 0.63 ± 0.25 |

nd, not determined.

* See MATERIALS AND METHODS for details.

We suggest that the clusters observed in mid-third-instar larvae are Golgi stack precursors with the use of two series of experiments. First, with the use of immunoelectron and confocal immunofluorescence microscopy, we show that the larval clusters contain Golgi markers, including dGM130 and dp115 that were colocalized with a newly described *Drosophila* Golgi protein, Fringe when it is expressed at low level. The immuno-EM was strongly indicative that these proteins were Golgi proteins (a labeling density ~10 times over background) although approximately one-third of the labeling was associated with the ER. This situation resembles closely the cellular distribution of *Drosophila* mannosidase II (Rabouille *et al.*, 1999) and could represent a characteristic of the *Drosophila* exocytic pathway. Second, we show that in different experimental designs the larval clusters are replaced by Golgi stacks of similar surface density, suggesting the conversion of the former into the latter without addition of new membrane structures. For instance, mid-third-instar larval clusters could rapidly be converted into small stacked Golgi cisternae when larvae were incubated at 37°C for 2 h. The possibility exists, however, that the clusters are consumed entirely to be replaced by Golgi stacks gener-

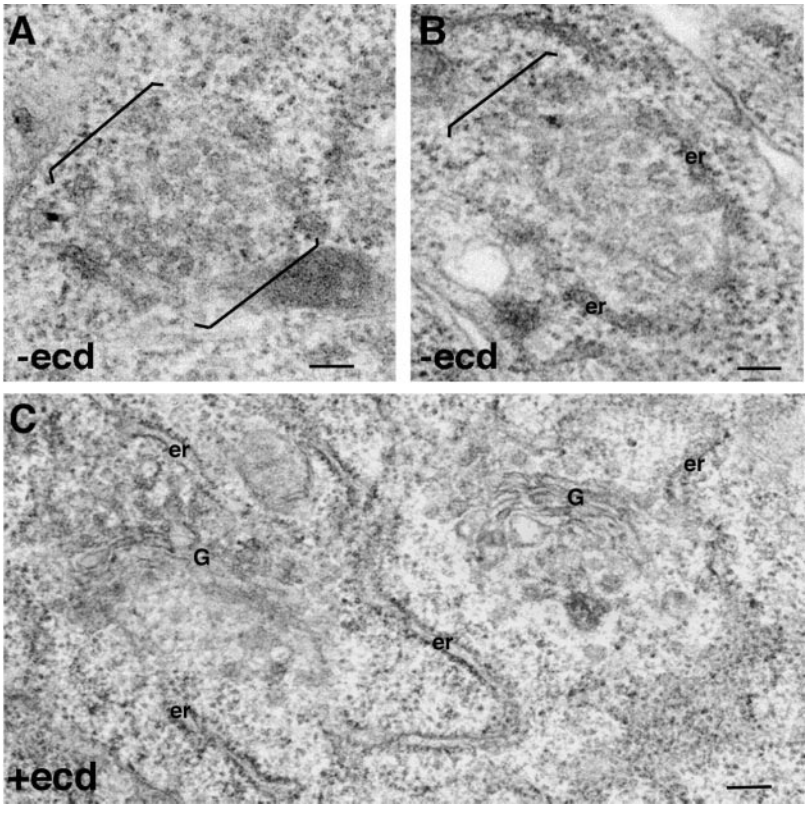


**Figure 8.** In vitro recapitulation of Golgi stack formation in the presence of ecdysone. WT mid-third-instar larvae were semidissected, incubated in M3 or Schneider medium either supplemented (C) with ecdysone and fly extract or without (A and B). Their discs were fixed and processed for conventional EM. The larval clusters and the Golgi areas are marked between brackets when ER cisternae are not marking the natural boundaries, and the stack marked with a G. er, endoplasmic reticulum. Bars, 100 nm.

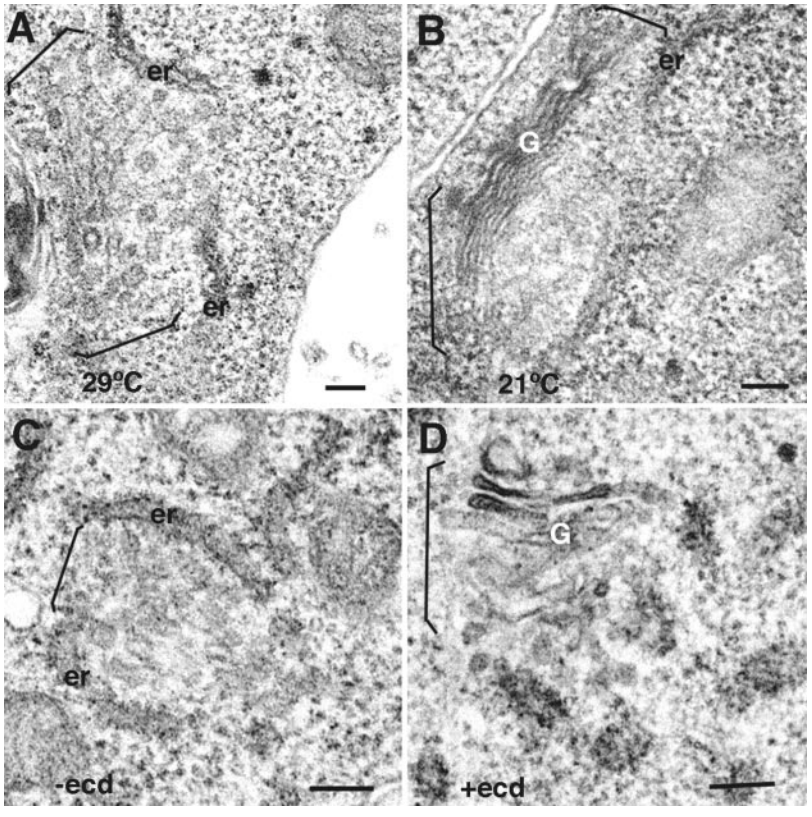


**Figure 9.** Effect of ecdysone on the Golgi stacks biogenesis. *ecd*$^{1ts}$ mutant larvae were maintained at the restrictive temperature of 29°C and either kept at 29°C (A) or released at 22°C for 18 h (B). Their disks were processed for EM and Golgi areas (either Golgi stacks or larval clusters) examined. Alternatively, *ecd*$^{1ts}$ mutant larvae maintained at 29°C were semidissected and incubated in the absence (C) or the presence (D) of 3 $\mu$M ecdysone. The larval clusters and the Golgi areas are marked between brackets when ER cisternae are not marking the natural boundaries, and the stack marked with a G. er, endoplasmic reticulum. Bars, 100 nm.

ated by a new independent mechanism. The conservation of surface density would then be coincidental. This situation seems to us unlikely. This conservation, though, also has been observed with the *ecd*$^{1ts}$ mutants. Furthermore, if the clusters would be consumed to be replaced by newly formed Golgi stacks, we would expect to see a disappearance of the clusters in situations where they cannot be converted, i.e., in the *comt 17* and *ecd*$^{1ts}$ mutants at restrictive temperature. Instead, we see the clusters remaining as clusters. The issue will only completely be resolved when real time experiments visualizing the membranes are carried out in a similar manner as in tissue culture cells (Mironov *et al.*, 2000).

We showed that dSec23p and dSec31p, the key components of the COPII machinery (Barlowe *et al.*, 1994; Schekman and Orci, 1996), are exhibiting a labeling pattern reminiscent of that of dGM130 and dp115 and overlap marginally with the ER. We found by immuno-EM that the larval clusters were labeled by Sec23 antibody (our unpublished results), and we also showed that dSec23p and dSec31p did colocalize substantially with Fringe (as dGM130 does), suggesting that the larval clusters derived primarily from the accumulation of COPII vesicles. This pattern is reminiscent of Sec13p colocalizing with Och1 in *Pichia pastoris* (Rossanese *et al.*, 2000). There were, however, a significant number of structures solely positive for dSec23p or dSec31p as well as structures solely positive for Fringe. This is the reflection of two types of limitations. First, cells did not express the same level of proteins and not all larval clusters within a cell were labeled to equivalent intensity. As a result, the overlap was variable and technically difficult to visualize. Second, the 20 or 40 min of heat shock necessary to induce Fringe expression also drove partially the conversion of some of the clusters into Golgi stacks (as in the WT type situation described in Figure 7B). Our preliminary immunoelectronmicroscopy results suggested that Fringe localized in the newly forming stacks, whereas dSec23p remained at the ER exit site as anticipated. These subtle localization differences could be picked up by immunofluorescence. This could also explain why dGM130, dp115, and Fringe show differential immunofluorescence patterns. Furthermore, it could also mean that not all ER exit sites are involved in the formation of larval clusters.

We found that the volume density of the larval clusters and the Golgi stacks within the cytoplasm increases from early third-instar larvae until white pupae, seemingly by accretion of newly formed vesicles. This observation suggests a mechanism whereby the dispersion of vesicles and tubules into the cytoplasm is prevented. They act as if they were anchored on a template or the "zone of exclusion" (Mollenhauer and Morré, 1978; Rabouille *et al.*, 1995b; Barr *et al.*, 1997). The anchoring of vesicles is thought to be an essential part of the formation of Golgi cisternae. It was shown in vitro that the concentration of mitotic Golgi fragments was a critical factor for their successful fusion to form cisternae (Rabouille *et al.*, 1995b). The anchoring template may play a similar role in vivo in achieving this critical concentration. Anchored vesicles would fuse together to form tubules and tubular networks, maybe under the form of vesicular tubular clusters described by Bannykh and Balch (1997). These vesicular tubular clusters would in turn

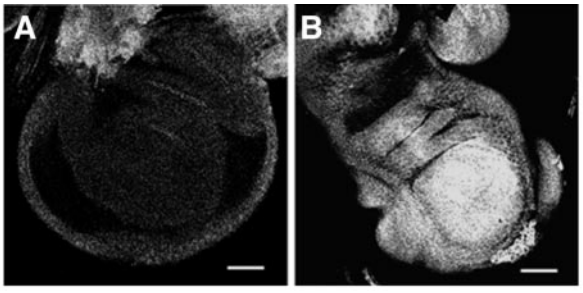


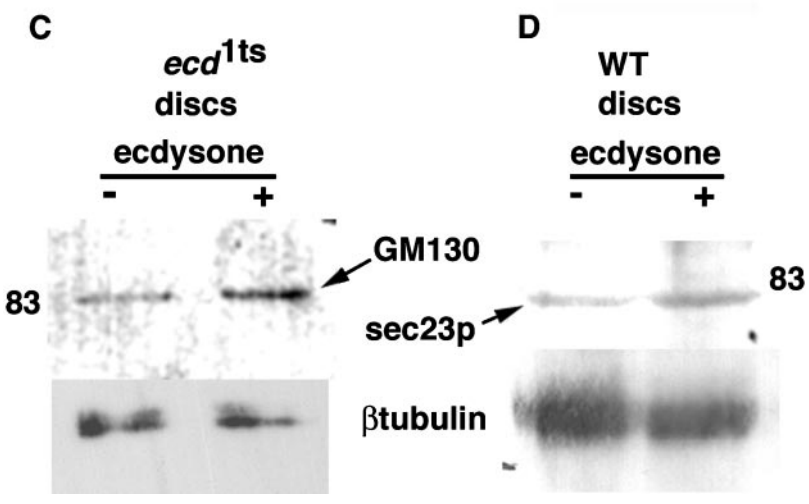


**Figure 10.** Effect of ecdysone on dGM130 and dSec23 protein expression. Mid- (A) and late (B) third-instar larval discs were immunolabeled with the use of MLO7 as described in Figures 3 and 5. (C) *ecd*$^{1ts}$ mutants were maintained at 29°C, their discs dissected and incubated at 22°C in the absence (−) or the presence (+) of 3 $\mu$M ecdysone for 18 h. Thirty leg and 10 wing discs were dissected from each incubation. Disc extract protein (30 $\mu$g) was loaded on each lane of a 10% acrylamide gel. Immunoblotting was performed with the use of the affinity-purified MLO7 and the mAb to $\beta$-tubulin. (D) Mid-third-instar WT larvae were semidissected and incubated in the absence (−) or in the presence (+) of 3 $\mu$M ecdysone. Sixty leg and 20 wing discs were dissected from each incubation. 60 $\mu$g of disc extract protein was loaded on each lane of a 10% acrylamide gel. Immunoblotting was performed with the use of the rabbit polyclonal antibody to Sec23p and the mAb to $\beta$-tubulin. Bar, 30 $\mu$m (A) and 40 $\mu$m (B).

undergo further fusion, leading to the formation of the first fenestrated cisterna that could perhaps then act as the template for the stacking of next newly made cisternae. Recent studies in *Pichia* have linked Golgi stacks formation to ER exit sites (tERs), which are discrete and contain Sec13 and Sec12. The *Pichia* tERs are specific regions of the ER, and they contain additional architectural components to those of *Saccharomyces cerevisiae* where no Golgi stacks are observed (Rossanese *et al.*, 2000). These additional components could build tER scaffolds.

The fusion ATPases (dNSF1 and TER94) are present in mid-third-instar larvae (our unpublished results). Our experimental evidence indeed suggests a role for dNSF1 in the fusion of small cluster fragments to form cisternae. When NSF was rendered nonfunctional, achieved with the use of the *comt 17* thermosensitive allele at restrictive temperature, the conversion of larval clusters in Golgi stacks did not take place. This phenotype was reverted by overexpressing dNSF1 in this mutant background, showing that the mutation in the dNSF1 gene was responsible for this phenotype. NSF has been shown to be involved in Golgi stack reassembly in two in vitro mammalian assays (Acharya *et al.*, 1995; Rabouille *et al.*, 1995a). That NSF is involved in Golgi stack biogenesis in our *Drosophila* system may suggest some similarities between the two processes, although the two systems do not recapitulate the same event. The in vitro assays dealt with the reassembly of the preexisting stacks of cisternae that were disassembled and subsequently reassembled, whereas we have described the growth of stacked cisternae from precursor membranes. The two processes, we think, have NSF in common. This result is also in agreement with the requirement of Sec18 (the yeast homolog of mammalian NSF) to drive the formation of Golgi stacks in *S. cerevisiae*, one of the other model systems currently exploited to study Golgi biogenesis (Morin-Ganet *et al.*, 2000).

*Comt 17* alleles have a point mutation that substitutes a glycine for an aspartic acid (G274E) in the D1 domain of the molecule. Our in vivo result is in good agreement with the results obtained by Müller *et al.* (1999) who showed that at 37°C the fusion of mitotic Golgi fragments in vitro was no longer supported by a chimeric mouse NSF cDNA in which an equivalent mutation G274E was introduced. This result is also in good agreement with the role of dNSF1 in neurotransmitter release (Tolar and Pallanck, 1998) at the nerve terminal. We do not know yet which SNAP receptors are involved. NSF has been shown to interact with numerous SNAP receptors, including syntaxin 5, Bet1p, membrin, Bos1p, Sec22p (synaptobrevin), and Gos28 (Klumperman, 2000). We could test the requirement of these molecules in the Golgi biogenetic event described here. The *Drosophila* Sec22 homologs has been cloned and Bet1, Gos28, and membrin have predicted homologs in *Drosophila* (Adams *et al.*, 2000), and there is a mutant for sed5 (Ashburner *et al.*, 1999) that we are currently using to address this issue.

The involvement of NSF in this conversion raises the question of the role of TER94. Two independent assays demonstrated that the reassembly of the Golgi stacks could be mediated by the NSF and by the p97 fusion machinery

(Acharya *et al.*, 1995; Rabouille *et al.*, 1995a). TER94 mutants are available and we are currently undertaking a series of experiments to address this question.

### *Ecdysone and Golgi Stack Biogenesis*

The timing of the morphological transition observed in the Golgi area suggested the possible involvement of 20-hydroxyecdysone, the steroid hormone known to trigger the morphogenetic event of puparium formation. We now have two lines of evidence suggesting that Golgi stack biogenesis occurring at the onset of disc elongation is influenced by ecdysone. With the use of the semidissected disc assay, the formation of Golgi stacks from larval clusters was observed in the presence of ecdysone. In contrast, in the absence of ecdysone, Golgi stack formation was prevented. In support of this finding mutant larvae $ecd^{1ts}$ exhibited a severely reduced conversion of larval clusters to Golgi stacks in vivo and in vitro. It seems that the ecdysone dependency of this biogenesis could shed light on its biological significance.

The possibility that the Golgi stack biogenesis is a mere consequence of the cellular events taking place under the control of ecdysone exists. For instance, cell rearrangement taking place during disc elongation could in turn drive Golgi stack formation. That Golgi stack biogenesis does not occur in the absence of ecdysone could simply be the result of the lack of disc elongation. To answer this question, it remains to be shown whether Golgi stack biogenesis precedes or is concomitant with disc elongation.

We have shown that the level of dGM130 increases by ~3 times from mid-to-late third-instar larvae. Ecdysone peaks at the late third-instar stage (~4–6 h before puparium formation) so the increased expression of dGM130 seems to be correlated with the ecdysone peak. We were able to show a causal relationship between the increased expression of dGM130 (~2.8-fold) and ecdysone with the use of discs from $ecd^{1ts}$ mutant larvae incubated in the presence of ecdysone. A similar result was obtained for dSec23p (increase of approximately fivefold) with the use of WT discs from mid-third-instar larvae incubated in vitro. That we only have shown this relationship at the protein level opens nevertheless to the exciting possibility that Golgi stack biogenesis is an event independently triggered by ecdysone at the gene expression level.

Recently, studies of gene expression regulated by ecdysone with the use of microarrays was published by White *et al.* (1999). Of ~6240 element-containing-sequences tested (including 4500 expressed sequence tags), 465 expressed sequence tags (10.3%) were ecdysone responsive and of these, 144 (3.2%) exhibited up-regulation. Interestingly, among these were the fusion ATPase TER94 (Rabouille *et al.*, 1995a) and the component of the COPII coat Sec23A (Barlowe *et al.*, 1994). We have also observed a strong up-regulation of dSec23p expression in our disc system induced by ecdysone and together with dGM130, could be the budding and anchoring components involved in building a Golgi apparatus. It remains to be seen whether the dGM130 gene and *dsec23* are a target for ecdysone and whether other genes encoding known proteins related to the Golgi apparatus are also responsive to ecdysone. We have results that suggest that there are such genes (Dunne and Rabouille, unpublished data). It will also be important to understand whether genes encoding these Golgi proteins are primary targets for ecdysone, and if not what are the transcription activators that mediate ecdysone activity.

The control of Golgi stack biogenesis by the hormone ecdysone would create a situation where the regulated synthesis of Golgi-related proteins stimulates its biogenesis. There are other cases of organelle biogenesis due to up-regulation of genes whose products are resident of this particular organelle. An example is the unfolded protein response (Cox and Walter, 1996). In yeast and mammalian systems, the amount of ER chaperone proteins increases dramatically when cells are exposed to stress. In yeast, a transducing mechanism exists by which the concentration of unfolded proteins in the ER is sensed by an ER transmembrane kinase, Ire1, which in turn leads to the raised stability of mRNA encoding ER chaperone proteins (Cox and Walter, 1996). Importantly, other pathways have also been shown to be targeted by the unfolded protein response (Ng *et al.*, 2000), including membrane lipid synthesis and the inositol response that may lead to ER biogenesis (Cox *et al.*, 1997).

The Golgi apparatus has also been shown to be remodeled during myogenesis. The Golgi apparatus occupies a juxtanuclear polarized organization in myoblasts and a perinuclear nonpolarized distribution in myotubes. In contrast, innervated muscle of chicks or mice displayed a focal distribution of the Golgi apparatus that appears restricted to areas located underneath the motor end plates in subneural domains (Jasmin *et al.*, 1989). Interestingly, some Golgi markers (e.g., α-mannosidase II, TGN 38) present in the embryonic myotubes are no longer detected in the innervated fiber even in the subsynaptic Golgi apparatus (Antony *et al.*, 1995). Our data and the results reported in this article suggest that specific developmental events can influence the Golgi organization. This is perhaps surprising because we were rather of the view that given the important place of the Golgi apparatus in the secretory pathway, its formation should be universal and uniform during development. This seems not to be the case and we might have now at hand one signal that triggers Golgi stack formation. Our task is to understand how the Golgi stack is built at the molecular level and how ecdysone controls this process.

### *Functional Biosynthetic Pathway*

The absence of stacked cisternae in third-instar larvae raises the issue of whether these cells possess a functional biosynthetic pathway. In the imaginal discs of third-instar larvae, many important patterning processes are taking place. The dorso/ventral and anterior/posterior regions are defined by secreted signaling molecules (Vincent, 1998) such as Dpp, Wingless and Hedgehog, and plasma membrane proteins such as Smo and Ptc. The cellular location of these proteins suggests one of two possibilities. Either the cells of third-instar larval discs possess a functional biosynthetic pathway in the absence of stacked cisternae, or these patterning molecules were exocytosed at an earlier developmental stage when Golgi stacks were perhaps present, and persisted into the third-instar larval stage where only clusters are observed. We are rather in favor of the notion that the larval clusters are functional. First, the equivalent Golgi clusters in salivary glands from early third-instar larvae are able to support the secretion of food digestive enzymes (Thomopoulos *et al.*, 1992). Second, we found that *comt 17* discs incubated at restrictive temperature did not elongate, prob-

ably because dNSF1 was not functional in supporting exocytosis (our unpublished results). Indeed, molecules whose lack of synthesis and transportation may inhibit disk elongation include the stubble gene product, IMP-E2 and -E3 (von Kalm *et al*., 1995) and integrins (Fristrom *et al*., 1993).

If larval clusters are functional, the question therefore remains as to why the Golgi morphology changes. It has been shown that the Golgi morphology changes when secretion increases (Rambourg *et al*., 1993). In *Drosophila* salivary glands, the conversion of Golgi clusters to stacks was observed concomitant to glue synthesis (Thomopoulos *et al*., 1992). A requirement for increased synthesis and secretion could explain the changes in Golgi morphology observed in larval imaginal discs. Furthermore, the formation of a polarized stack could ensure proper differential oligosaccharide or protein processing and targeting, crucial for one or more particular unidentified proteins involved in disk elongation, or for the further synthesis of pupal cuticle that has a different composition to larval cuticle (Riddiford, 1993). Regardless of the explanation, the biogenesis of Golgi stacks at puparium formation seems to be a regulated event triggered by ecdysone.

## ACKNOWLEDGMENTS

We thank Leo Pallanck (Washington) for the gift of HSN transgenic lines; Barry Ganetzky for the *comt 17* allele; Matthew Freeman (Cambridge, United Kingdom) for the gift of the UAS-Fringe-DXD-myc fly line (stock 919); J.A. Lepesant (Paris, France) for the gift of the *ecd*$^{1ts}$ mutant; Martin Lowe (Manchester, United Kingdom) for the gift of the MLO7 and NN7 antibodies, and for helpful comments on the manuscript; David Vaux (Oxford, United Kingdom) for the gift of the 1D3 antibody; Carol Lyons (Dundee, United Kingdom) for the anti-ribophorin I antibody; Jean Pierre Paccaud (Geneva, Switzerland) for antibody to Sec23p; Fred Gorelick (Yale, NJ) for antibody to Sec31p; Neil White (Edinburgh, United Kingdom) for the use of an embryonic cDNA library; Julie Diplexcito for cloning *Drosophila* p115; members of the Davis, Heck, Jarman, and Okhura labs for help with the flies; Marcel van den Heuvel and France Docquier for teaching and support; Graham Warren for helpful discussions; and Ken Sawin and Marcel van den Heuvel for critical comments on the manuscript. We acknowledge the use of fly base (http://flybase.bio.indiana.edu) and the Berkeley *Drosophila* Genome Project (http://www.fruitfly.org) Web sites. This study was funded by the Medical Research Council.

## REFERENCES

Acharya, U., Jacobs, R., Peters, J.M., Watson, N., Farquhar, M.G., and Malhotra, V. (1995). The formation of Golgi stacks from vesiculated Golgi membranes requires two distinct fusion events. Cell *82*, 895–904.

Acharya, U., Mallabiabarrena, A., Acharya, J.K., and Malhotra, V. (1998). Signaling via mitogen-activated protein kinase kinase (MEK1) is required for Golgi fragmentation during mitosis. Cell *92*, 183–192.

Adams, M.D., et al. (2000). The genome sequence of *Drosophila melanogaster*. Science *287*, 2185–2195.

Antony, C., Huchet, M., Changeux, J.P., and Cartaud, J. (1995). Developmental regulation of membrane traffic organization during synaptogenesis in mouse diaphragm muscle. J. Cell Biol. *130*, 959–968.

Ashburner, M. et al. (1999). An exploration of the sequence of a 2.9-Mb region of the genome of *Drosophila melanogaster*: the Adh region. Genetics *153*, 179–219.

Banfield, D.K., Lewis, M.J., Rabouille, C., Warren, G., and Pelham, H.R. (1994). Localization of Sed5, a putative vesicle targeting molecule, to the cis-Golgi network involves both its transmembrane and cytoplasmic domains. J. Cell Biol. *127*, 357–371.

Bannykh, S.I., and Balch, W.E. (1997). Membrane dynamics at the endoplasmic reticulum-Golgi interface. J. Cell Biol. *138*, 1–4.

Barlowe, C., Orci, L., Yeung, T., Hosobuchi, M., Hamamoto, S., Salama, M., Rexach, M.F., Ravazzola, M., Amherdt, M., and Schekman, R. (1994). COP II - a membrane coat formed by sec proteins that drive vesicle budding from the endoplasmic-reticulum. Cell *77*, 895–907.

Barr, F.A., Puype, M., Vandekerckhove, J., and Warren, G. (1997). GRASP65, a protein involved in the stacking of Golgi cisternae. Cell *91*, 253–262.

Bruckner, K., Perez, L., Clausen, H., and Cohen, S. (2000). Glycosyltransferase activity of Fringe modulates Notch-Delta interactions. Nature *406*, 411–415.

Cox, J.S., Chapman, R.E., and Walter, P. (1997). The unfolded protein response coordinates the production of endoplasmic reticulum protein and endoplasmic reticulum membrane. Mol. Biol. Cell *8*, 1805–1814.

Cox, J.S., and Walter, P. (1996). A novel mechanism for regulating activity of a transcription factor that controls the unfolded protein response. Cell *87*, 391–404.

Currie, D.A., Milner, M.J., and Evans, C.W. (1988). The growth and differentiation in vitro of leg and wing imaginal disc cells from *Drosophila melanogaster*. Development *102*, 805–814.

Dirac-Svejstrup, A.B., Shorter, J., Waters, M.G., and Warren, G. (2000). Phosphorylation of the vesicle-tethering protein p115 by a casein kinase II-like enzyme is required for Golgi reassembly from isolated mitotic fragments. J. Cell Biol. *150*, 475–487.

Dunne, J., and Rabouille, C. (2001). Lord of the flies: the Golgi in development. In: The ELSO Gazette: e-magazine of the European Life Scientist Organization (http://www.the-elso-gazette/magazines/issue3/mreviews/mreviews1.asp), issue 3 (January 1, 2001).

Fristrom, D., and Fristrom, J.W. (1993). The metamorphic development of the adult epidermis. In: The Development of *Drosophila melanogaster*, vol II, ed. M. Bates and A. Martinez Arias, Cold Spring Harbor, NY: Cold Spring Harbor Laboratory Press, 843–897.

Fristrom, D., Wilcox, M., and Fristrom, J. (1993). The distribution of PS integrins, laminin A and F-actin during key stages in *Drosophila* wing development. Development *117*, 509–523.

Fullilove, S.L., and Jacobson, A.G. (1971). Nuclear elongation and cytokinesis in *Drosophila montana*. Dev. Biol. *26*, 560–577.

Jasmin, B.J., Cartaud, J., Bornens, M., and Changeux, J.P. (1989). Golgi apparatus in chick skeletal muscle: changes in its distribution during end plate development and after denervation. Proc. Natl. Acad. Sci. USA *86*, 7218–7222.

Garen, A., Kauvar, L., and Lepesant, J.A. (1977). Role of ecdysone in *Drosophila* development. Proc. Natl. Acad. Sci. USA *74*, 5099–5103.

Hui, N., Nakamura, N., Sonnichsen, B., Shima, D.T., Nilsson, T., and Warren, G. (1997). An isoform of the Golgi t-SNARE, syntaxin 5, with an endoplasmic reticulum retrieval signal. *8*, 1777–1787.

Klumperman, J. (2000). Transport between ER and golgi. Curr. Opin. Cell Biol. *12*, 445–449.

Kondo, H., Rabouille, C., Newman, R., Levine, T.P., Pappin, D., Freemont, P., and Warren, G. (1997). p47 is a cofactor for p97-mediated membrane fusion. Nature *388*, 75–78.

Lecuit, T., and Wieschaus, E. (2000). Polarized insertion of new membrane from a cytoplasmic reservoir during cleavage of the *Drosophila* embryo. J. Cell Biol. *150*, 849–860.

Leon, A., and McKearin, D. (1999). Identification of TER94, an AAA ATPase protein, as a Bam-dependent component of the *Drosophila* fusome. Mol. Biol. Cell *10*, 3825–3834.

Lowe, M., Rabouille, C., Nakamura, N., Watson, R., Jackman M, Jämsa, E., Rahman, D., Pappin, D.J., and Warren, G. (1998). Cdc2 kinase directly phosphorylates the cis-Golgi matrix protein GM130 and is required for Golgi fragmentation in mitosis. Cell *94*, 783–793.

Mandaron, P. (1971). Mechanism of imaginal disk evagination in *Drosophila*. Dev. Biol. *25*, 581–605.

Martinez-Menarguez, J.A., Geuze, H.J., Slot, J.W., and Klumperman, J. (1999). Vesicular tubular clusters between the ER and Golgi mediate concentration of soluble secretory proteins by exclusion from COPI-coated vesicles. Cell *98*, 81–90.

McKay, R.R., Zhu, L., and Shortridge, R.D. (1995). A *Drosophila* gene that encodes a member of the protein disulfide isomerase/phospholipase C-alpha family. Insect Biochem. Mol. Biol. *25*, 647–654.

Mironov, A.A., Polishchuk, R.S., and Luini, A. (2000). Visualizing membrane traffic in vivo by combined video fluorescence and 3D electron microscopy. Trends Cell Biol. *10*, 349–353.

Mollenhauer, H.H., and Morré, D.J. (1978). Structural compartmentation of the cytosol: zones of exclusion, zones of adhesion, cytoskeletal and intercisternal elements. Subcell. Biochem. *5*, 327–359.

Morin-Ganet, M.N., Rambourg, A., Deitz, S.B., Franzusoff, A., and Képès, F. (2000). Morphogenesis and dynamics of the yeast Golgi apparatus. Traffic *1*, 56–68.

Müller, J.M.M., Rabouille, C., Newman, R., Shorter, J., Freemont, P., Schiavo, G., Warren, G., and Shima, D.T. (1999). An NSF function distinct from ATPase-dependent SNARE disassembly is essential for Golgi membrane fusion. Nat. Cell Biol. *1*, 335–340.

Munro, S., and Freeman, M. (2000). The Notch signaling regulator fringe acts in the Golgi apparatus and requires the glycosyltransferase signature motif DXD. Curr. Biol. *10*, 813–820.

Nakamura, N., Lowe, M., Levine, T.P., Rabouille, C., and Warren, G. (1997). The vesicle docking protein p115 binds GM130, a cis-Golgi matrix protein, in a mitotically regulated manner. Cell *89*, 445–455.

Nakamura, N., Rabouille, C., Watson, R., Nilsson, T., Hui, N., Slusarewicz, P., Kreis, T.E., and Warren, G. (1995). Characterization of a cis-Golgi matrix protein, GM130. J. Cell Biol. *131*, 1715–1726.

Nilsson, T., Pypaert, M., Hoe, M.H., Slusarewicz, P., Berger, E.G., and Warren, G. (1993). Overlapping distribution of two glycosyltransferases in the Golgi apparatus of HeLa cells. J. Cell Biol. *120*, 5–13.

Ng, D.T.W., Spear, E.D., and Walter, P. (2000). The unfolded protein response regulates multiple aspects of secretory and membrane protein biogenesis and endoplasmic reticulum quality control. J. Cell Biol. *150*, 77–88.

Oprins, A., Duden, R., Kreis, T.E., Gueze, H.J., and Slot, J.W. (1993). b-COP localizes mainly to the cis-Golgi side in exocrine pancreas. J. Cell Biol. *121*, 49–59.

Orci, L., Perrelet, A., Ravazolla, M., Amherdt, M., Rothman, J.E., and Schekman, R. (1994). Coatomer-rich endoplasmic-reticulum. Proc. Natl. Acad. Sci. USA *91*, 11924–11928.

Ordway, R.W., Pallanck, L. and Ganetzky, B. (1994). Neurally expressed *Drosophila* genes encoding homologs of the NSF and SNAP secretory proteins. Proc. Natl. Acad. Sci. USA *91*, 5715–5719.

Pallanck, L., Ordway, R.W., and Ganetzky, B. (1995a). A *Drosophila* NSF mutant. Nature *376*, 25.

Pallanck, L., Ordway, R.W. Ramaswami, M., Chi, W.Y., Krishnan, K.S., and Ganetzky, B. (1995b). Distinct roles for N-ethylmaleimide-sensitive fusion protein (NSF) suggested by the identification of a second *Drosophila* homologue. J. Biol. Chem. *270*, 18742–18744.

Paccaud, J.P., Reith, W., Carpentier, J.L., Ravazzola, M., Amherdt, M., Schekman, R., and Orci, L. (1996). Cloning and functional characterization of mammalian homologues of the COPII component Sec23. Mol. Biol. Cell, *7*, 1535–1546.

Pinter, M., Jenely, G., Szepesi, R.J., Farkas, A., Theopold, U., Meyer, H.E., Lindholm, D., Nassel, D.R., Aultmark, D., and Friedrich, P. (1998). TER94, a *Drosophila* homolog of the membrane fusion protein CDC48/p97, is accumulated in nonproliferating cells, in the reproductive organs and in the brain of the imago. Insect Biochem. Mol. Biol. *28*, 91–98.

Rabouille, C. (1999). Quantitative aspects of immunogold labeling in embedded and nonembedded sections. Methods Mol. Biol. *117*, 125–144.

Rabouille, C., Kondo, H., Newman, R., Hui, N., Freemont, P., and Warren, G. (1998). Syntaxin 5 is a common component of the NSF- and p97-mediated reassembly pathways of Golgi cisternae from mitotic Golgi fragments in vitro. Cell *92*, 603–610.

Rabouille, C., Kuntz, D.A., Lockyer, A., Watson, R., Signorelli, T., Rose, D.R., van den Heuvel, M., and Roberts, D.B. (1999). The *Drosophila* GMII gene encodes a Golgi $\alpha$-mannosidase II. J. Cell Sci. *112*, 3319–3330.

Rabouille, C., Levine, T.P., Peters, J.M., and Warren, G. (1995a). An NSF-like ATPase, p97, and NSF mediate cisternal regrowth from mitotic Golgi fragments. Cell *82*, 905–914.

Rabouille, C., Misteli, T., Watson, R., and Warren, G. (1995b). Reassembly of Golgi stacks from mitotic Golgi fragments in a cell-free system. J. Cell Biol. *129*, 605–618.

Rambourg, A., Clermont, Y., Chretien, M., and Olivier, L. (1993). Modulation of the Golgi apparatus in stimulated and nonstimulated prolactin cells of female rats. *235*, 353–362.

Redfern, C.P.F., and Bownes, M. (1983). Pleitropic effects of the "ecdysoneless-1" mutation of *Drosophila melanogaster*. Mol. Gen. Genet. *189*, 432–440.

Riddiford, L.M. (1993). Hormones and *Drosophila* development. In: The Development of *Drosophila melanogaster*, vol II. ed. M. Bates and A. Martinez Arias, Cold Spring Harbor, NY: Cold Spring Harbor Laboratory Press, 843–897.

Ripoche, J., Link, B., Yucel, J.K., Tokuyasu, K., and Malhotra, V. (1994). Location of Golgi membranes with reference to dividing nuclei in syncytial *Drosophila* embryos. Proc. Natl. Acad. Sci. USA *91*, 1878–1882.

Rossanese, O., Soderholm, J., Bevis, B.J., Sears, I.B., O'Connor, J., Williamson, E.K., and Glick, B.S. (2000). Golgi structure correlates with transitional endoplasmic reticulum organization in *Pichia pastoris* and *Saccharomyces cerevisiae*. J. Cell Biol. *145*, 69–81.

Schekman, R., and Orci, L. (1996). Coat proteins and vesicle budding. Science *271*, 1526–1533.

Shorter, J., Watson, R., Giannakou, M.E., Clarke, M., Warren, G., and Barr, F.A. (1999). GRASP55, a second mammalian GRASP protein involved in the stacking of Golgi cisternae in a cell-free system. EMBO J. *18*, 4949–4960.

Sisson, J.C., Field, C., Ventura, R., Royou, A., and Sullivan, W. (2000). Lava lamp. a novel peripheral Golgi protein, is required for *Drosophila melanogaster* cellularisation. J. Cell Biol. *151*, 905–918.

Siddiqi, O., and Benzer, S. (1976). Neurophysiological defects in temperature-sensitive paralytic mutants of *Drosophila melanogaster*. Proc. Natl. Acad. Sci. USA *73*, 3253–3257.

Simpson, F., Peden, A.A., Christodoulou, L., and Robinson, M.S. (1997). Characterization of the adaptor-related protein complex, AP-3. J. Cell Biol. *137*, 835–845.

Shugrue, C.A., Kolen, E.R., Peters, H., Czernik, A., Kaiser, C., Matovcik, L., Hubbard, A.L., and Gorelick, F. (1999). Identification of

the putative mammalian orthologue of Sec31P, a component of the COPII coat. J. Cell Sci. *112*, 4547–4556.

Stanley, H., Botas, J., and Malhotra, V. (1997). The mechanism of Golgi segregation during mitosis is cell type-specific. Proc. Natl. Acad. Sci. USA *94*, 14467–14470.

Thomopoulos, G.N., Neophytou, E.P., Alexiou, M., Vadolas, A., Limberi-Thomopoulos, S., and Derventzi, A. (1992). Structural and histochemical studies of Golgi complex differentiation in salivary gland cells during *Drosophila* development. J. Cell Sci. *102*, 169–184.

Tolar, L.A., and Pallanck, L. (1998). NSF function in neurotransmitter release involves rearrangement of the SNARE complex downstream of synaptic vesicle docking. J. Neurosci. *18*, 10250–10256.

Vaux, D., Tooze, J., and Fuller, S. (1990). Identification by anti-idiotype antibodies of an intracellular membrane protein that recognizes a mammalian endoplasmic reticulum retention signal. Nature *345*, 495–502.

Vincent, J.P. (1998). Compartment boundaries: where, why and how? Int. J. Dev. Biol. *42*, 311–315.

von Kalm, L., Fristrom, D., and Fristrom, J.W. (1995). The making of a fly leg: a model for epithelial morphogenesis. Bioessays *17*, 693–702.

White, K.P., Rifkin, S.A., Hurban, P., and Hogness, D.S. (1999). Microarray analysis of *Drosophila* development during metamorphosis. Science *286*, 2179–2184.

Yoshihisa, T., Barlowe, C., and Scheckman, R. (1993). Requirement for a GTPase activating protein in vesicle budding from the endoplasmic reticulum. Science *259*, 1466–1468.